

GPS System Segments

Arthur J. Dorsey and Willard A. Marquis
Lockheed Martin Corporation

Peter M. Fyfe
The Boeing Company

Elliott D. Kaplan and Lawrence F. Wiederholt
The MITRE Corporation

3.1 Overview of the GPS System

GPS is comprised of three segments: satellite constellation, ground-control/monitoring network, and user receiving equipment. Formal GPS JPO programmatic terms for these components are space, control, and user equipment segments, respectively. The satellite constellation is the set of satellites in orbit that provide the ranging signals and data messages to the user equipment. The control segment (CS) tracks and maintains the satellites in space. The CS monitors satellite health and signal integrity and maintains the orbital configuration of the satellites. Furthermore, the CS updates the satellite clock corrections and ephemerides as well as numerous other parameters essential to determining user PVT. Finally, the user receiver equipment (i.e., user segment) performs the navigation, timing, or other related functions (e.g., surveying). An overview of each system segment is provided next, followed by further elaboration on each segment starting in Section 3.2.

3.1.1 Space Segment Overview

The space segment is the constellation of satellites from which users make ranging measurements. The SVs (i.e., satellites) transmit a PRN-coded signal from which the ranging measurements are made. This concept makes GPS a passive system for the user with signals only being transmitted and the user passively receiving the signals. Thus, an unlimited number of users can simultaneously use GPS. A satellite's transmitted ranging signal is modulated with data that includes information that defines the position of the satellite. An SV includes payloads and vehicle control subsystems. The primary payload is the navigation payload used to support the GPS PVT mission; the secondary payload is the nuclear detonation (NUDET) detection system, which supports detection and reporting of Earth-based radiation phenomena.

The vehicle control subsystems perform such functions as maintaining the satellite pointing to Earth and the solar panels pointing to the Sun.

3.1.2 Control Segment (CS) Overview

The CS is responsible for maintaining the satellites and their proper functioning. This includes maintaining the satellites in their proper orbital positions (called stationkeeping) and monitoring satellite subsystem health and status. The CS also monitors the satellite solar arrays, battery power levels, and propellant levels used for maneuvers. Furthermore, the CS activates spare satellites (if available) to maintain system availability. The CS updates each satellite's clock, ephemeris, and almanac and other indicators in the navigation message at least once per day. Updates are more frequently scheduled when improved navigation accuracies are required. (Frequent clock and ephemeris updates result in reducing the space and control contributions to range measurement error. Further elaboration on the effects of frequent clock and ephemeris updates is provided in Sections 3.3.1.4 and 7.2).

The ephemeris parameters are a precise fit to the GPS satellite orbits and are valid only for a time interval of 4 hours with the once-per-day normal upload schedule. Depending on the satellite block, the navigation message data can be stored for a minimum of 14 days to a maximum of a 210-day duration in intervals of 4 hours or 6 hours for uploads as infrequent as once per two weeks and intervals of greater than 6 hours in the event that an upload cannot be provided for over 2 weeks. The almanac is a reduced precision subset of the ephemeris parameters. The almanac consists of 7 of the 15 ephemeris orbital parameters. Almanac data is used to predict the approximate satellite position and aid in satellite signal acquisition. Furthermore, the CS resolves satellite anomalies, controls SA and AS (see Sections 1.3.1 and 7.2.1), and collects pseudorange and carrier phase measurements at the remote monitor stations to determine satellite clock corrections, almanac, and ephemeris. To accomplish these functions, the CS is comprised of three different physical components: the master control station (MCS), monitor stations, and the ground antennas, each of which is described in more detail in Section 3.3.

3.1.3 User Segment Overview

The user receiving equipment comprises the user segment. Each set of equipment is typically referred to as a *GPS receiver*, which processes the L-band signals transmitted from the satellites to determine user PVT. While PVT determination is the most common use, receivers are designed for other applications, such as computing user platform attitude (i.e., heading, pitch, and roll) or as a timing source. Section 3.4 provides further discussion on the user segment.

3.2 Space Segment Description

The space segment has two principal aspects: One aspect is the constellation of satellites in terms of the orbits and positioning within the orbits. The other aspect is the features of the satellites that occupy each orbital slot. Each aspect is described next.

3.2.1 GPS Satellite Constellation Description

The U.S. government baseline configuration for the constellation consists of 24 satellites. Within this configuration, the satellites are positioned in six Earth-centered orbital planes with four satellites in each plane. The nominal orbital period of a GPS satellite is one-half of a sidereal day or 11 hours, 58 minutes [1]. The orbits are nearly circular and equally spaced around the equator at a 60° separation with a nominal inclination relative to the equatorial plane of 55° . Figure 3.1 depicts the GPS constellation. The orbital radius (i.e., nominal distance from the center of mass of the Earth to the satellite) is approximately 26,600 km. This satellite constellation provides a 24-hour global user navigation and time determination capability. Figure 3.2 presents the satellite orbits in a planar projection referenced to the epoch time of 0000h July 1, 1993 UTC (USNO). Thinking of an orbit as a ring, this figure opens each orbit and lays it flat on a plane. Similarly, for the Earth's equator, it is like a ring that has been opened and laid on a flat surface. The slope of each orbit represents its inclination with respect to the Earth's equatorial plane, which is nominally 55° .

The orbital plane locations with respect to the Earth are defined by the longitude of the ascending node, while the location of the satellite within the orbital plane is defined by the mean anomaly. The longitude of the ascending node is the point of intersection of each orbital plane with the equatorial plane. The Greenwich meridian is the reference point where the longitude of the ascending node has the value of zero. Mean anomaly is the angular position of each satellite within the orbit, with the Earth's equator being the reference or point with a zero value of mean anomaly. It can be observed that the relative phasing between most satellites in adjoining orbits is approximately 40° . The Keplerian parameters for the 24-SV constellation are defined in Section 2.3.1.

The orbital slot assignments of this baseline design are contained in [2] and are provided in Table 3.1. (Note that RAAN is the Right Ascension of the Ascending Node, as defined in Section 2.3.1.)

The remaining reference orbit values (with tolerances) are:

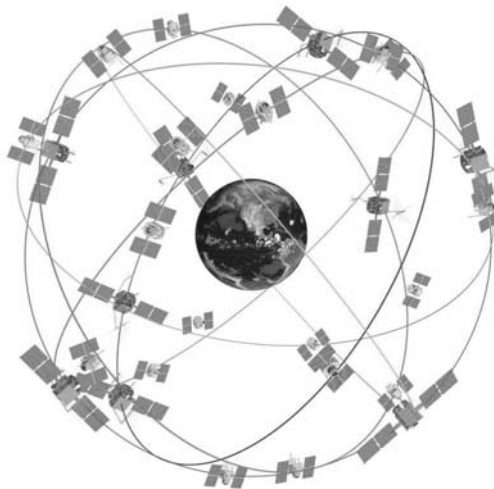


Figure 3.1 GPS satellite constellation. (Source: Lockheed Martin Corp. Reprinted with permission.)

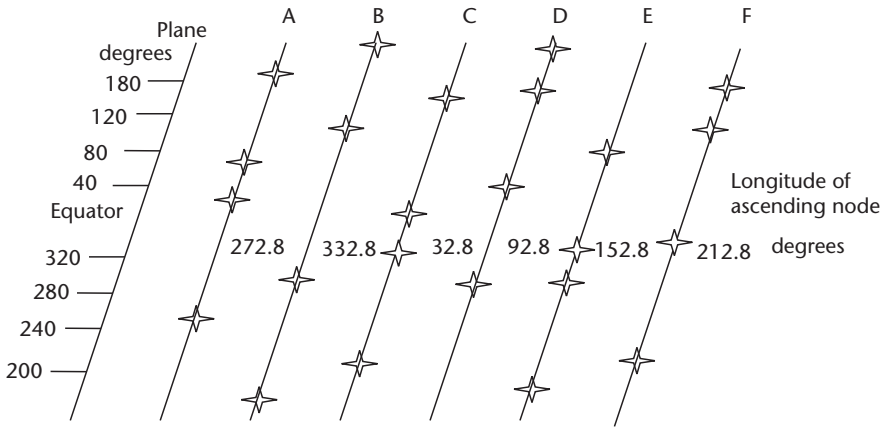


Figure 3.2 GPS constellation planar projection.

Table 3.1 Reference Orbit Slot Assignments as of the Defined Epoch

Slot	RAAN (°)	Argument of Latitude (°)	Slot	RAAN (°)	Argument of Latitude (°)
A1	272.847	268.126	D1	92.847	135.226
A2	272.847	161.786	D2	92.847	265.446
A3	272.847	11.676	D3	92.847	35.136
A4	272.847	41.806	D4	92.847	167.356
B1	332.847	80.956	E1	152.847	197.046
B2	332.847	173.336	E2	152.847	302.596
B3	332.847	309.976	E3	152.847	66.066
B4	332.847	204.376	E4	152.847	333.686
C1	32.847	111.876	F1	212.847	238.886
C2	32.847	11.796	F2	212.847	345.226
C3	32.847	339.666	F3	212.847	105.206
C4	32.847	241.556	F4	212.847	135.346

Defined epoch: 0000Z, July 1, 1993; Greenwich hour angle: 18 hours, 36 minutes, 14.4 seconds referenced to FK5/J2000.00 coordinates.

- Groundtrack equatorial crossing: $\pm 2^\circ$;
- Eccentricity: 0.00–0.02;
- Inclination: $55^\circ \pm 3^\circ$;
- Semimajor axis: 26,559.7 km \pm 50 km for Block IIR, \pm 17 km for Block II/IIA;
- Longitude of the ascending node: $\pm 2^\circ$;
- Argument of perigee: $\pm 180^\circ$.

Several different notations are used to refer to the satellites in their orbits. One nomenclature assigns a letter to each orbital plane (i.e., A, B, C, D, E, and F) with each satellite within a plane assigned a number from 1 to 4. Thus, a satellite referenced as B3 refers to satellite number 3 in orbital plane B. A second notation used is a NAVSTAR satellite number assigned by the U.S. Air Force. This notation is in the

form of space vehicle number (SVN); for example, 60 refers to NAVSTAR satellite 60. The third notation represents the configuration of the PRN code generators onboard the satellite. These PRN code generators are configured uniquely on each satellite, thereby producing unique versions of both C/A code and P(Y) code. Thus, a satellite can be identified by the PRN codes that it generates. Occasionally, the PRN assignment for a given SVN can change during the satellite's mission duration.

3.2.2 Constellation Design Guidelines

As discussed in Section 2.3.2, several tradeoffs are involved in the design of the GPS constellation. One primary concern is the geometric contribution to navigation accuracy; in other words, is the satellite geometry sufficiently diverse to provide good observability to users throughout the world. This geometry is measured by a parameter called dilution of precision (DOP) and is described in more detail in Section 7.3. Studies continue concerning tradeoffs on different possible satellite configurations. Some studies have investigated the use of 30 satellites in three orbital planes as well as the utility of geostationary satellites. Most of this work is done with a nominal constellation assuming all satellites are healthy and operational, but a new dimension for study is introduced when satellite failures are considered. Single or multiple satellite failures provide a new dimension around which to optimize performance from a geometry consideration. Another design consideration is line-of-sight observability of the satellites by the ground stations to maintain the ephemeris of the satellites and the uploading of this data.

3.2.3 Space Segment Phased Development

The continuing development of the control and space segments has been phased in over many years, starting in the mid-1970s. This development started with a concept validation phase and has progressed to several production phases. The satellites associated with each phase of development are called a *block* of satellites. Characteristics of each phase and block are presented in the following sections.

3.2.3.1 Satellite Block Development

Five satellite blocks have been developed to date. The initial concept validation satellites were called Block I. The last remaining prototype Block I satellite was disposed of in late 1995. Block II satellites are the initial production satellites, while Block IIA refers to upgraded production satellites. All Block I, II, and IIA satellites have been launched. Block IIR satellites, denoted as the replenishment satellites, are being deployed. At the time of this writing, modified Block IIR versions denoted as Block IIR-M were scheduled for launch in 2005. Block IIF satellites, referred to as the follow-on or sustainment satellites, are being built. GPS III satellites are in the planning stage for a post-2010 deployment. Since satellites are launched only as replacements for a satellite failure, their scheduling is difficult to predict, especially when most satellites have far outlived their design lifetime. At the time of this writing, the constellation consisted of 27 operational satellites. Table 3.2 describes the configuration of the current satellite constellation. Thus, the current optimized con-

stellation has up to seven orbital slots unevenly spaced around each plane, with some satellites in relatively close proximity to provide redundant coverage for near-term predicted failures. Since the state of the constellation varies, the Internet is the best source for current status information. One such Web site is operated and maintained by the U.S. Coast Guard Navigation Center [3].

3.2.3.2 Navigation Payload Overview

The navigation payload is responsible for the generation and transmission of ranging codes and navigation data on the L1, L2, and (starting with Block IIF) L5 carrier frequencies to the user segment. Control of the navigation payload is taken from

Table 3.2 Satellite Constellation Configuration (as of January 29, 2005)

<i>Block/Launch Order</i>	<i>PRN Number</i>	<i>SVN</i>	<i>Launch Date</i>	<i>Orbital Slot</i>
II-5	17	17	December 11, 1989	D6
II-9	15	15	October 1, 1990	D5
IIA-11	24	24	July 4, 1991	D1
IIA-12	25	25	February 23, 1992	A2
IIA-14	26	26	July 7, 1992	F2
IIA-15	27	27	September 9, 1992	A4
IIA-16	01	32	November 22, 1992	F6
IIA-17	29	29	December 18, 1992	F5
IIA-19	31	31	March 30, 1993	C5
IIA-20	07	37	May 13, 1993	C4
IIIA-21	09	39	June 26, 1993	A1
IIA-22	05	35	August 30, 1993	B4
IIA-23	04	34	October 26, 1993	D4
IIA-24	06	36	March 10, 1994	C1
IIA-25	03	33	March 28, 1996	C2
IIA-26	10	40	July 16, 1996	E3
IIA-27	30	30	September 12, 1996	B2
IIA-28	08	38	November 6, 1997	A3
IIR-2	13	43	July 23, 1997	F3
IIR-3	11	46	October 7, 1999	D2
IIR-4	20	51	May 11, 2000	E1
IIR-5	28	44	July 16, 2000	B3
IIR-6	14	41	November 10, 2000	F1
IIR-7	18	54	January 30, 2001	E4
IIR-8	16	56	January 29, 2003	B1
IIR-9	21	45	March 31, 2003	D3
IIR-10	22	47	December 21, 2003	E2
IIR-11	19	59	March 20, 2004	C3
IIR-12	23	60	June 23, 2004	F4
IIR-13	02	61	November 6, 2004	D7

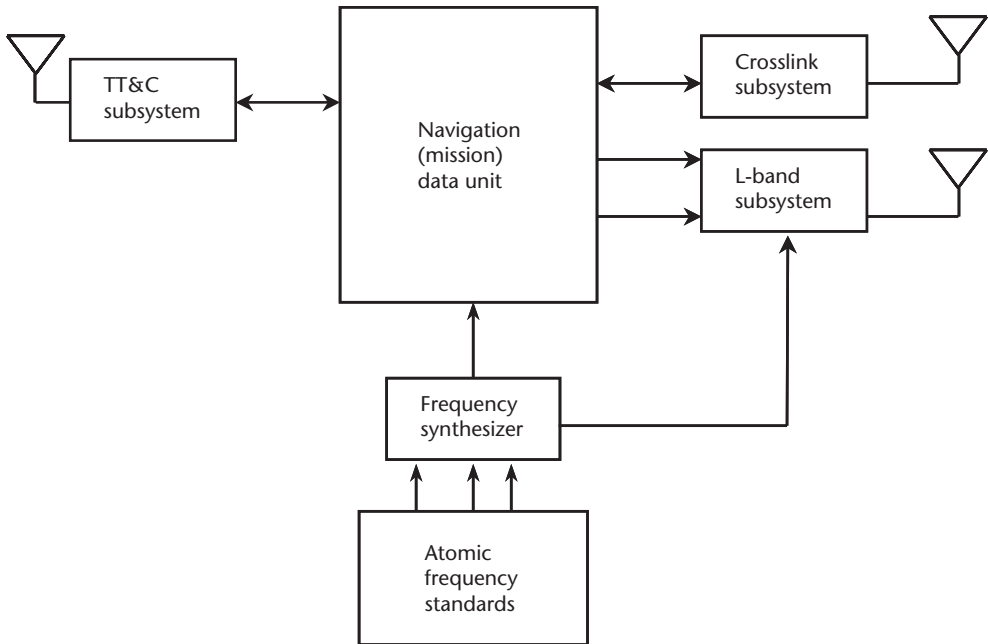


Figure 3.3 Satellite navigation payload.

reception of the predicted navigation data and other control data from the CS via the tracking, telemetry, and control (TT&C) links. The navigation payload is only one part of the spacecraft, with other systems being responsible for such functions as attitude control and solar panel pointing. Figure 3.3 is a generic block diagram of a navigation payload. Atomic frequency standards (AFSs) are used as the basis for generating the extremely stable ranging codes and carrier frequencies transmitted by the payload. Each satellite contains multiple AFSs to meet the mission reliability, with only one operating at any time. Since the AFSs operate at their natural frequencies, a frequency synthesizer, phase-locked to the AFS, generates the basic 10.23-MHz reference that serves as the timing reference within the payload for ranging signal and transmit frequency generation. The navigation data unit (NDU), known as the mission data unit in the Block IIR design, contains the ranging code generators that generate the C/A code and P(Y) codes (plus new civil and military signals in later payloads) for modulo-2 addition with the navigation message data. The NDU also contains a processor that stores the uploads received from the CS containing multiple days of navigation message data, and it assures that the current issue of navigation message data is provided for this modulo-2 addition. The combined baseband ranging signals are then sent to the L-band subsystem where they are modulated onto the L-band carrier frequencies and amplified for transmission to the user. (Chapter 4 describes the signal-generation process in detail.) The L-band subsystem contains numerous components, including the L1 and L2 transmitters and associated antenna. The NDU processor also interfaces to the crosslink receiver/transmitter for intersatellite communication, as well as ranging, on Block IIR and later versions. This crosslink receiver/transmitter uses a separate antenna and feed system. (It should be noted that the intersatellite ranging is functional on the Block IIR, Block IIR-M, and Block IIF space vehicles; however, the U.S. govern-

ment has chosen so far not to add this capability to the CS.) As stated previously, the primary and secondary SV payloads are navigation and NUDET, respectively. Occasionally, the satellites carry additional payloads, such as laser reflectors for satellite laser ranging (i.e., validation of predicted ephemeris), and free electron measurement experiments.

3.2.3.3 Block I—Initial Concept Validation Satellites

Block I satellites were developmental prototypes to validate the initial GPS concept, so only 11 satellites were built. The Block I satellites, built by Rockwell International, were launched between 1978 and 1985 from Vandenberg Air Force Base, California. A picture of the Block I satellite is presented in Figure 3.4. The onboard storage capability was for about 3.5 days of navigation messages. The navigation message data was transmitted for a 1-hour period and was valid for an additional 3 hours. Since there was no onboard momentum dumping, frequent ground contact was required for momentum management. Without momentum dumping, the satellites would lose attitude control after a short time interval. Two cesium and two rubidium AFSs were employed. These satellites were designed for a mean mission duration (MMD) of 4.5 years, a design life of 5 years and inventory expendable (e.g., fuel, battery life, and solar panel power capacity) of 7 years. Reliability improvements were made to the atomic clocks on later satellites based on failure analysis from earlier launches. Some Block I satellites operated for more than double their design life.

3.2.3.4 Block II—Initial Production Satellites

On-orbit operation of the Block I satellites provided valuable experience that led to several significant capability enhancements in subsystem design for the Block II operational satellites. These improvements included radiation hardening to prevent random memory upset from such events as cosmic rays to improve reliability and survivability. Besides these enhancements, several other refinements were incorporated to support the fully operational GPS system requirements. Since the NDU processor would not be programmable on-orbit, flexibility was designed into the flight



Figure 3.4 Block I satellite.

software via changeable databases. Thus, no reprogramming has been required on the Block II satellites since the first launch. While most of the changes affected only the CS/space interface, some also affected the user signal interface. The significant changes are identified as the following: To provide security, SA and AS capabilities were added. (SA and AS are discussed in Sections 1.3.1 and 7.2.1.) System integrity was improved by the addition of automatic error detection for certain error conditions. After detection of these error conditions, there is a changeover to the transmission of nonstandard PRN codes (NSCs) to prevent the usage of a corrupted signal or data. Nine Block II satellites were built by Rockwell International, and the first was launched in February 1989 from Cape Canaveral Air Force Station in Florida. The onboard navigation message storage capacity was expanded to allow for a 14-day mission. Autonomous onboard momentum control was implemented in the satellite within the attitude and velocity control system, thus eliminating the need for ground contact to perform momentum dumping. Again, for reliability and survivability, multiple rubidium and cesium AFSs were onboard. These satellites were designed for a MMD of 6 years, a design life of 7.5 years, and inventory expendables (e.g., fuel, battery life, and solar panel power capacity) of 10 years. At the time of this writing, one Block II satellite remained in the constellation. The Block II average life to date is 11.8 years, with SVN 15 having the greatest longevity at nearly 15 years. Figure 3.5 depicts a Block II satellite.

3.2.3.5 Block IIA—Upgraded Production Satellites

The Block IIA satellites are very similar to the Block II satellites, but with a number of system enhancements to allow an extended operation period of 180 days. Spacecraft autonomous momentum control was extended. The onboard navigation data storage capability was tested to assure retention for the 180-day period. For approximately the first day on-orbit, the navigation message data is broadcast for a

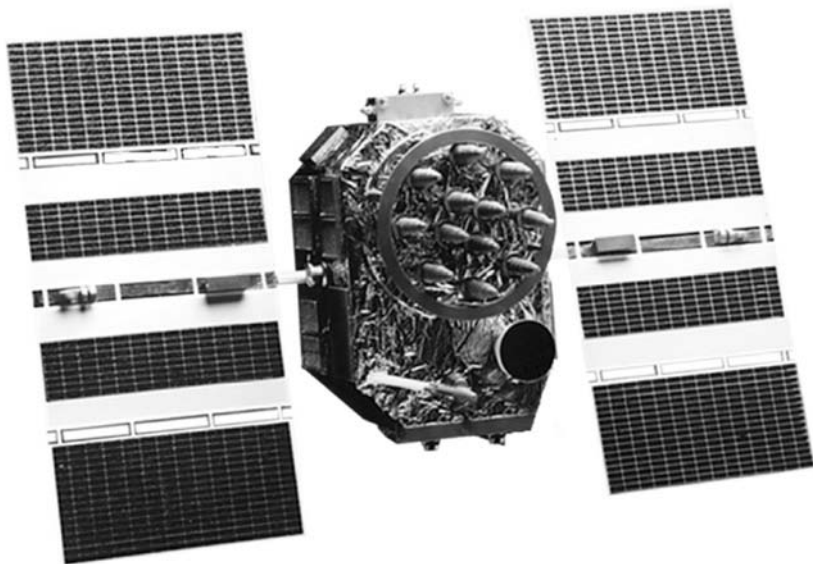


Figure 3.5 Block II satellite.

2-hour period and is valid over a 4-hour interval. For the remainder of the first 14 days, the navigation message is broadcast for a 4-hour period with a validity period of 6 hours (2 additional hours). Following this initial 14-day period, the navigation message data broadcast periods gradually extend from 6 hours to 144 hours. With this additional onboard storage retention capability, the satellites can function continuously for a period of 6 months without ground contact. However, the accuracy of the CS ephemeris and clock predictions and thus the accuracy of the navigation message data gracefully degrade over time such that the user range error (URE) will be bounded by 10,000m after 180 days. (The URE is the contribution of the pseudorange error from the CS and space segment.) Typically, the URE is 1.4m (1σ). (Pseudorange errors are extensively discussed in Section 7.2.) With no general onboard processing capability, no updates to stored reference ephemeris data are possible. So, as a result, full system accuracy is only available when the CS is functioning properly and navigation messages are uploaded on a daily basis. Block IIA electronics are radiation-hardened. Nineteen Block IIA satellites were built by Rockwell International, with the first launched in November 1990 from Cape Canaveral Air Force Station in Florida and the last launched in November 1997. The life expectancy of the Block IIA is the same as that of the Block II. At the time of this writing, 16 Block IIA satellites remained in the constellation, with a projected MMD of over 10.3 years. A Block IIA satellite is shown in Figure 3.6.

3.2.3.6 Block IIR—Replenishment Satellites

The GPS Block IIR (replenishment) satellites (Figure 3.7) represent an ever-growing presence in the GPS constellation. Over half of the original 21 IIR SVs have been



Figure 3.6 Block IIA satellite.



Figure 3.7 Block IIR satellite. (Source: Lockheed Martin Corp. Reprinted with permission.)

launched since 1997 (the first Block IIR satellite was lost in a launch accident early that year). Lockheed Martin and its navigation payload subcontractor, ITT Aerospace/Communications, are building these satellites.

The Block IIR began development following contract award in 1989 as a totally compatible upgrade and replacement to the Block II and Block IIA SVs. All of the basic GPS features are supported: C/A and P(Y) code on L1, P(Y) on L2, ultra-high frequency (UHF) crosslink capability, attitude determination system to stabilize the SV bus platform, reaction control system to maintain the on-orbit location in the constellation, and sufficient power capacity for the life of the vehicle.

There are two versions of the Block IIR SV. The “classic” IIR and its AFSs, autonomy, reprogrammability, and improved antenna panel will be described first. The features of the “modernized” IIR will be covered later in this section.

Classic IIR

The baseline (nonmodernized) GPS Block IIR has now been dubbed the *classic IIR*.

The Block IIR satellites are designed for a MMD of 6 years, a design life of 7.5 years, and inventory expendables (e.g., fuel, battery life, and solar panel power capacity) of 10 years. As of August 2005, there were 12 IIR SVs in the 30-SV constellation. The oldest IIR SV (SVN 43) was over 8 years old at time of this writing, exceeding the required 7.5-year design life.

Figure 3.8 shows some of the main components of the Block IIR SV. Several of these will be highlighted in the remainder of this section.

Advanced Atomic Frequency Standards

All IIR SVs contain three next generation rubidium AFSs (RAFS). The IIR design has a significantly enhanced physics package that improves stability and reliability [4].

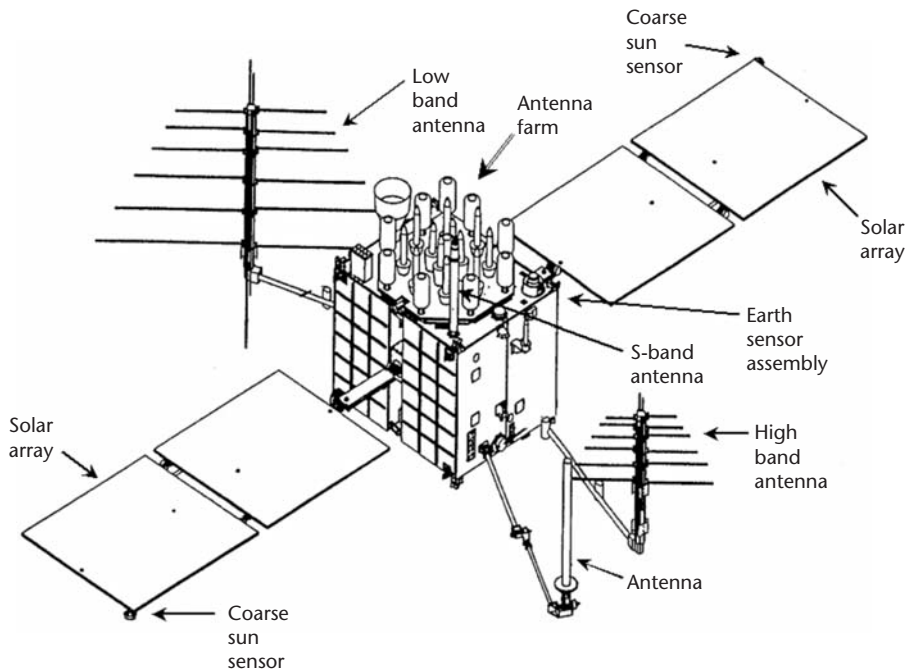


Figure 3.8 Block IIR satellite components. (Source: Lockheed Martin Corp. Reprinted with permission.)

The RAFS has a MMD of 7.5 years. It is coupled with a redundant voltage controlled crystal oscillator (VCXO) and software functionality into what is called the time keeping system (TKS). The TKS loop provides a timing tuning capability to stabilize and control satellite clock performance.

IIR Accuracy

An accurate onboard AFS provides the key to good GPS PVT accuracy [5]. Figure 3.9 shows the 1-day Hadamard deviation for mid-2004. Hadamard deviation measures frequency stability—the lower the number, the more stable the AFS. Hadamard deviation (as opposed to Allan deviation) currently provides the best way to measure frequency stability in AFS with nonzero frequency drift. (Appendix B provides descriptions of both the Hadamard and Allan deviations.)

The IIR specification requires that the total IIR URE (defined in Section 3.2.3.5) value should be less than 2.2m when operating a RAFS. The URE performance for GPS IIR has averaged approximately 0.8m or better for several years [6]. Thus, the required specification is easily surpassed.

There is also a significantly improved solar pressure model (by an order of magnitude compared to the II/IA model) used in the MCS when computing the orbit of the IIR [7, 8]. This increases the accuracy of the ephemeris modeling on the ground.

Enhanced Autonomy

The advanced capabilities of the Block IIR SV include a redundancy management system called REDMAN, which monitors bus subcomponent functionality and provides for warning and component switching to maintain SV health.

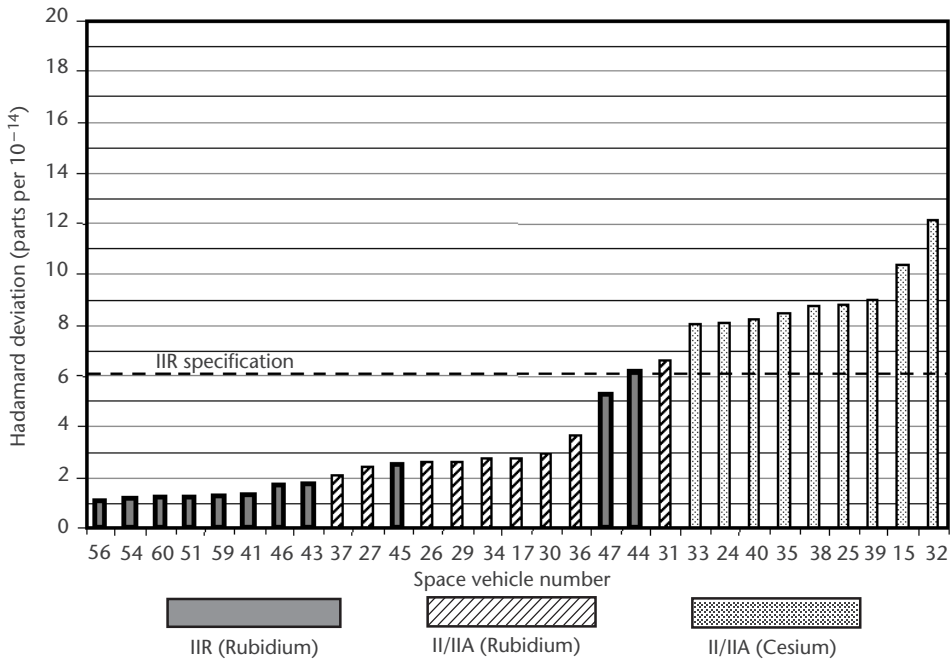


Figure 3.9 One-day Hadamard stability ranking. (Source: Lockheed Martin Corp. Reprinted with permission.)

The Block IIR uses nickel hydrogen (NiH_2) batteries, which require no reconditioning and accompanying operator burden.

When in Earth eclipse, automatic pointing of the solar array panels is accomplished via an onboard orbit propagation algorithm to enable quiescent reacquisition of the Sun following eclipse exit. This provides a more stable and predictive SV bus platform and orientation for the L-band signal.

Block IIR has an expanded NSC capability to protect the user from spurious signals. It is enabled automatically in response to the detection of the most harmful on-orbit RAFS and VCXO discontinuities.

Block IIR has a capability to perform autonomous navigation via intersatellite crosslink ranging. This function is called AutoNav. It provides 180-day independent navigation performance without ground contact. Although the CS currently cannot support full AutoNav operation, portions of this capability are undergoing on-orbit testing. There is potential for increased accuracy when using AutoNav.

In addition to intersatellite ranging, other communications with on-orbit SVs consist of crosslink commanding and data transfer to other SVs in the constellation. The Block IIR SVs were also designed to operate through laser and nuclear threats.

Reprogrammability

There are several reprogrammable computers on board: the redundant SV bus spacecraft processor unit (SPU) and the redundant navigation system mission data unit (MDU). Reprogrammability allows the CS to change the flight software in on-orbit SVs. This feature has already been employed on-orbit in several instances. The MDU was provided with diagnostic buffers to give detailed insight into the behavior of the TKS. It was also given a jumpstart capability allowing current TKS

parameters to be saved to a special area of memory and reused following the load of a new program. This feature reduces, by about 4 hours, the time required to recover from a new program load. The SPU was provided with new rolling buffers to save high-speed telemetry data for SV functions even when not in contact with the CS.

Improved Antenna Panel

Lockheed Martin, under an internal research and development effort, developed new L-band and UHF antenna element designs. The new L1 power received on the ground will be at least -154.5 dBW (edge-of-Earth, as compared to the current typical IIR performance of -155.5 dBW) and the new L2 power received on the ground will be -159.5 dBW (edge-of-Earth, as compared to the current typical IIR performance of -161.5 dBW). This provides greater signal power to the user. The last 4 of the 12 classic IIRs and all of the modernized IIRs have the improved antenna panel.

Block IIR-M-Modernized Replenishment Satellites

The modernized GPS IIR (IIR-M) (see Figure 3.10) will bring new services to military and civilian users [9, 10]. The IIR-M is the result of an effort to bring modernized functionality to IIR SVs that were built several years ago and placed into storage until they were needed for launch. The Air Force contracted Lockheed Martin in 2000 to modernize several of the unlaunched IIR SVs. This modernization program has been accomplished within existing solar array capability, available on-board processor margins, and current vehicle structural capabilities.

As many as eight Block IIR SVs will be modernized. Maintaining constellation health could interfere with this goal, but current predictions are optimistic as the

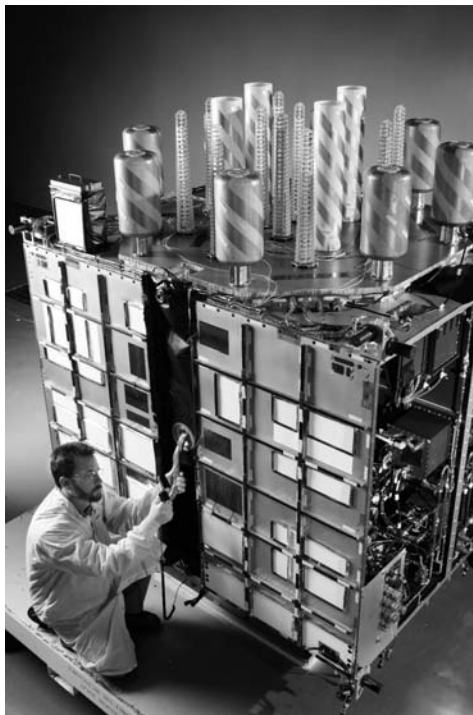


Figure 3.10 Block IIR-M satellite. (Source: Lockheed Martin Corp. Reprinted with permission.)

older Block II/IIA SVs continue to surprise with their longevity. IIR-M brings the new military and civilian services to users at least 3 years earlier than if modernized capabilities were to wait for just Block IIF and Block III.

At the time of this writing, the IIR-M SVs were undergoing the design modifications and were available for launch in 2005. Early testing of L2C and M code (new civil and military signals, respectively) will occur for some time following the first IIR-M launch while more modernized SVs are added to the constellation.

Modernized Signals

New L-band signals and increased L-band power will significantly improve navigation performance for users worldwide. Three new signals will be provided: two new military codes on L1 and on L2, and a new civilian code on L2. The new L2 civil signal denoted as L2C will be an improved signal sequence over L1 C/A, enabling ionospheric error correction to be done by civilian users. It will be ground-selectable, allowing selection of either L2 C/A or a proposed new L2C code or L2C off. The new signal structure will be totally backward-compatible with existing L1 C/A and P(Y), and L2 P(Y). (Refer to Section 4.5.1 for further details.)

The M code on L1 and L2 for the military user will also be ground-selectable and will include a pseudo-M code to be used during testing activities. The new M code will provide the authorized user with more signal security.

Modernized Hardware

The new navigation panel boxes consist of a redesigned L1 transmitter, a redesigned L2 transmitter, and the new waveform generator/modulator/intermediate power amplifier/converter (WGMIC) (Figure 3.11). The WGMIC is a new box developed by ITT coupling the brand-new waveform generator with the functionality of the L1 signal modulator/intermediate power amplifier (IPA), the L2 signal modulator/IPA, and the dc-to-dc converter. The waveform generator provides much of the new modernized signal structure and controls the power settings on the new transmitters. To manage the thermal environment of these higher-power boxes, heat pipes were incorporated into the fabrication of the structural panel. Lockheed Martin has used similar heat pipes on other satellites it has built.

The improved IIR antenna panel discussed earlier in this section will also be installed on all IIR-M SVs. This will provide greater signal power to the user. The antenna redesign effort was begun prior to the modernization decision but will significantly enhance the new IIR-M features. L-band power will be increased on both L1 and L2 frequencies. L1 will be increased by at least double the power, and L2 will be increased by at least quadruple power at low elevation angles.

The UHF performance has also been improved. This does not directly affect the user, but it enhances intersatellite communication: data transfer, commanding, and crosslink ranging.

Other total navigation payload (TNP) modifications include new MDU software that is also useable in the classic IIR SVs. Table 3.3 highlights some of the other SV modifications, including the new antenna array (which includes the downlink signal L-band array), new power switching capability, as well as other component and harness changes.

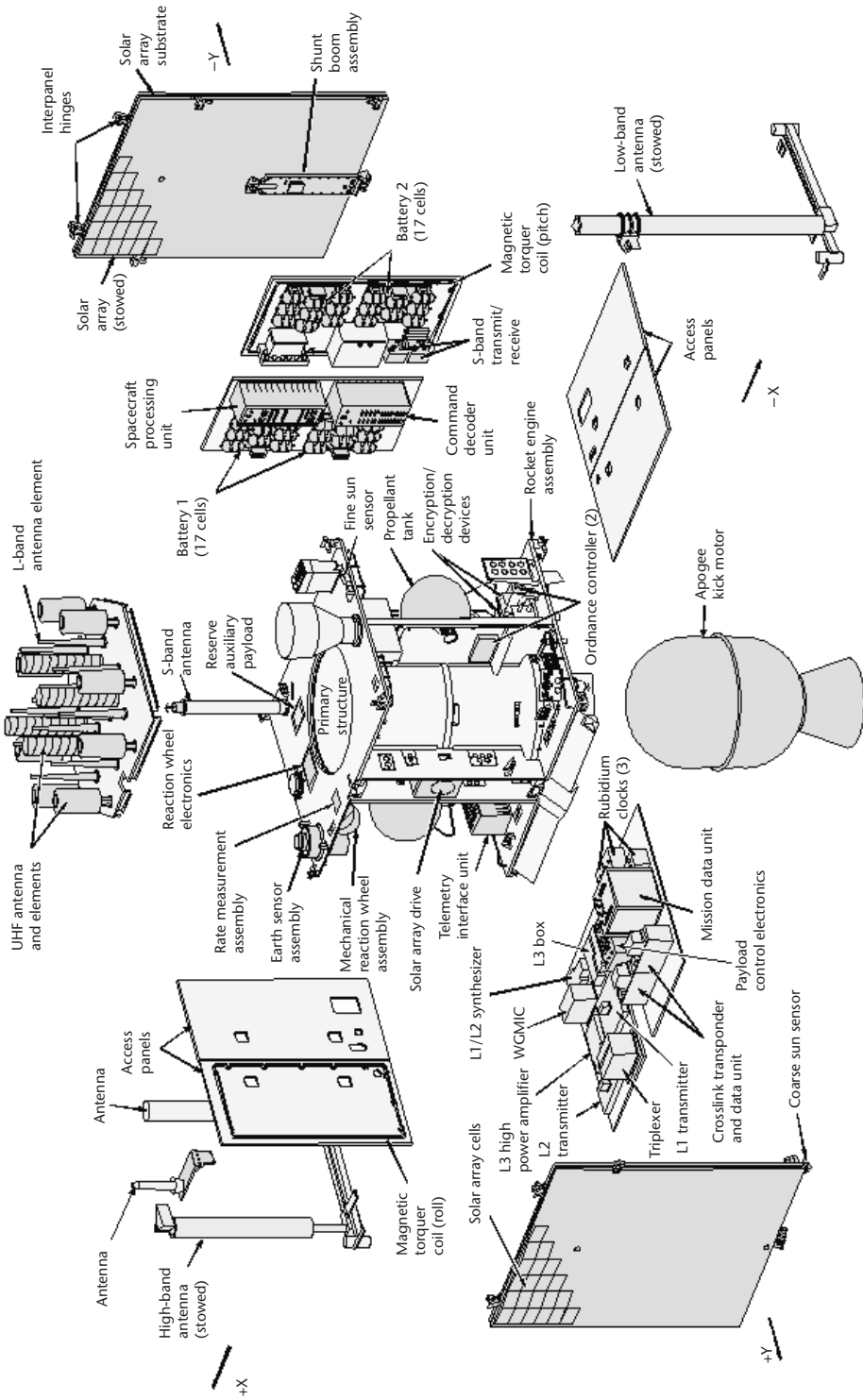


Figure 3.11 Block IIR-M expanded view. (Source: Lockheed Martin Corp. Reprinted with permission.)

Table 3.3 IR-M Modification Summary

<i>Component</i>	<i>Magnitude of Change</i>	<i>Description of Change</i>
Antenna panel	Moderate redesign	Replace L-band elements with broadband proprietary elements
L-band subsystem	Technology upgrade	Replace five separate components with three multifunction assemblies (L1 and L2 high-power amplifiers and a WGMIC)
L-band structural panel	New design, similar to those flown on communication SVs	Higher-power dissipation requires integral heat pipes in the panel honeycomb structure
Payload control electronics	Minor modification	Add power switching and fusing to accommodate additional power
Power regulation unit	Minor modification	Spare pins connected to additional power and return lines for higher power

3.2.3.7 Block IIF—Follow-On Sustainment Satellites

In 1995, the Air Force (GPS JPO) released a request for proposal (RFP) for a set of satellites to sustain the GPS constellation, designated as Block II follow-on, or IIF. The RFP also requested the provider to include the modifications to the GPS CS necessary to operate the IIF SV. While necessary for service sustainment, the IIF SV procurement afforded the Air Force the opportunity to start adding new signals and additional flexibility to the system beyond the capabilities and improvements of the IIR SV. A new military acquisition code on L2 was required, as well as an option for a new civil L5 signal at a frequency within 102.3 MHz of the existing L2 frequency of 1,227.6 MHz. The L5 frequency that was eventually settled upon was 1,176.45 MHz, placing it in a frequency band that is protected for ARNS. (The L5 signal is described in Section 4.5.2.)

The RFP also allowed the provider to offer additional “best value” features that could be considered during the proposal evaluation. Boeing (then Rockwell) included several best value features in its proposal and was awarded the IIF contract in April 1996. Several of these features were to improve service performance, including a URE 3m or less in AutoNav mode, an age of data for the URE of less than 3 hours using the UHF crosslink to update the navigation message, and design goals for AFS Allan variance performance better than specification. (Appendix B contains details on the Allan variance.) Other features supported the addition of auxiliary payloads on the IIF SV and reduction of operational complexity for the operators via greater use of the UHF crosslink communication system.

The original planned launch date for the first IIF SV was April 2001. However, due to the longevity of the Block II and IIA SVs and projected service life of the IIR SVs, the need date for a IIF launch was extended sufficiently to allow the Air Force to direct modifications to the IIF SV that resulted in the present design. The first modification was enabled when the Delta II launch vehicle (LV) was deselected for IIF, leaving the larger evolved expendable launch vehicle (EELV) as the primary LV. The larger fairing of the EELV enabled the “Big Bird” modification to the IIF SV, which expanded the spacecraft volume, nadir surface area, power generation, and thermal dissipation capability. Around the same time, extensive studies were performed by the GPS Modernization Signal Development Team (GMSDT) to evaluate

new capabilities needed from GPS, primarily to add new military and civil ranging signals. The GMSDT was formed as a government/Federally Funded Research and Development Center (FFRDC)/industry team to evaluate the deficiencies of the existing signal structure and recommend a new signal structure that would address the key areas of modulation and signal acquisition, security, data message structure, and system implementation. Today’s M code signal structure is the result of those studies. (M code is discussed in Section 4.5.3.) The complete list of ranging signals provided by the IIF SV is shown in Table 3.4. It should be noted that the new ranging signals also carry improved versions of the clock and ephemeris data in their respective navigation messages. This eliminates some of the resolution limitations the original navigation message had imposed as the URE has continued to improve.

The original flexibility and expandability features of the IIF SV in both the spacecraft and navigation payload designs allowed the addition of these new signals without major revisions to the IIF design. An exploded view of the Block IIF SV is depicted in Figure 3.12. The figure shows all of the components of the spacecraft subsystems. These include the attitude determination and control subsystem, which keeps the antennas pointing at the Earth and the solar panels at the Sun; the electrical power subsystem that generates, regulates, stores, and shunts the DC power for the satellite; and the TT&C subsystem, which allows the MCS operators to communicate with and control the satellite on-orbit. To support the increase in DC power requirements due to the increased transmit power, the solar arrays were switched from silicon technology to higher efficiency triple-junction gallium arsenide. Additionally, the thermal design had to be revised to accommodate the additional transmitter thermal loads. Other than some realignment to maintain weight and thermal balance, no other modifications were required for the spacecraft.

The navigation payload on the Block IIF SV includes two RAFSs and one cesium AFS per the contract requirement for dual technology. These AFSs provide the tight frequency stability necessary to generate high-accuracy ranging signals. The NDU generates all of the baseband forms of the ranging signals. The original NDU design included a spare slot that allowed the addition of M code and the L5 signal within the same envelope. The original NDU computer was designed with 300% expansion memory margin and 300% computational reserve (throughput margin), so that there was sufficient reserve to support the generation of the new navigation messages for M code and L5 plus other modernization requirements. The computer program is reprogrammable on-orbit and is loaded from onboard electrically erasable programmable read-only memory (EEPROM) when power is applied, avoiding the need for large blocks of contact time with the ground antennas. The L-band subsystem generates about 350W of radio frequency (RF) power for transmitting the three sets of signals in Table 3.4.

Table 3.4 Block IIF Ranging Signal Set

<i>Link (Frequency)</i>	L1 (1,575.42 MHz)	L2 (1,227.6 MHz)	L5 (1,176.45 MHz)
<i>Open (civil) signals</i>	C/A code P(Y) code	L2C P(Y) code	L5
<i>Military (restricted) signals</i>	M code	M code	—

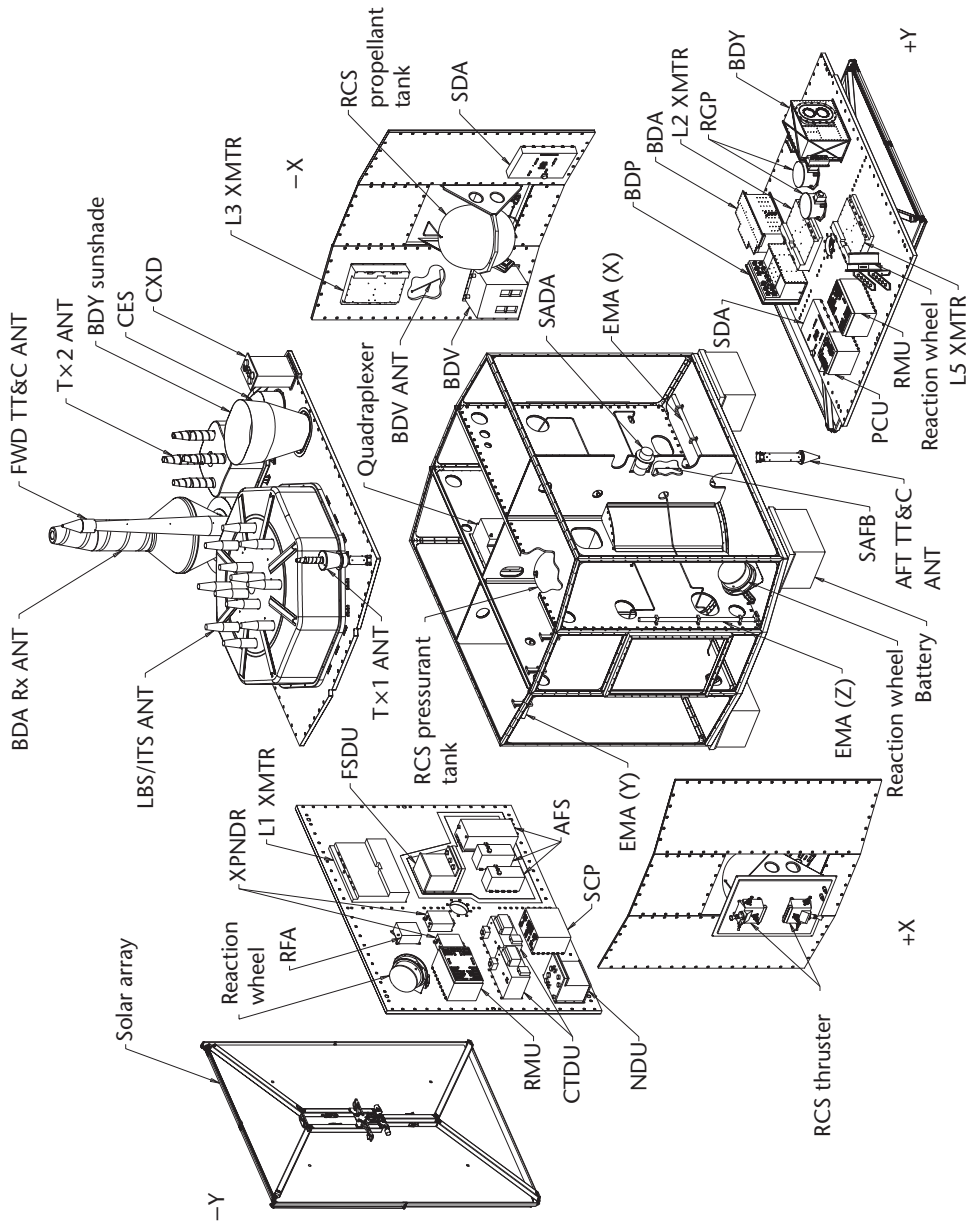


Figure 3.12 Expanded view of the Block IIF. (Source: The Boeing Company. Reprinted with permission.)

The Block IIF SV is designed for a life of 12 years with a MMD of 9.9 years. It is backward compatible with the Block IIR capabilities described in Section 3.2.3.6, including the capability to operate in AutoNav mode. An on-orbit depiction of the Block IIF SV is shown in Figure 3.13. The nadir-facing side contains a set of UHF and L-band antennas and other components that are very reminiscent of all of the previous GPS satellites.

The original IIF contract was for a basic buy of 6 SVs and two options of 15 and 12 SVs for a possible total of 33 SVs. At the time of this writing, GPS JPO projections indicated that 16 Block IIF SVs will be procured and launched to maintain the constellation prior to the start of GPS III. The first Block IIF launch is scheduled for 2007.

3.2.3.8 Block III—Next Generation Satellites

The GPS III program was conceived to reassess the entire GPS architecture as it has evolved to its present state and determine the correct architecture to lead into the future. The program has two main goals: reduce the government's total ownership costs and provide sufficient architectural flexibility to satisfy evolving requirements through 2030. On a more technical side, GPS III is expected to provide submeter position accuracy, greater timing accuracy, a system integrity solution, a high data capacity intersatellite crosslink capability, and higher signal power to meet military anti-jam requirements. Two system architecture/requirements development (SARD) studies were performed in 2001–2002 by contractor teams led by Boeing and Lockheed Martin, resulting in a baseline concept description from each team. (An unfunded study was conducted by Spectrum Astro.) After a short extension on those

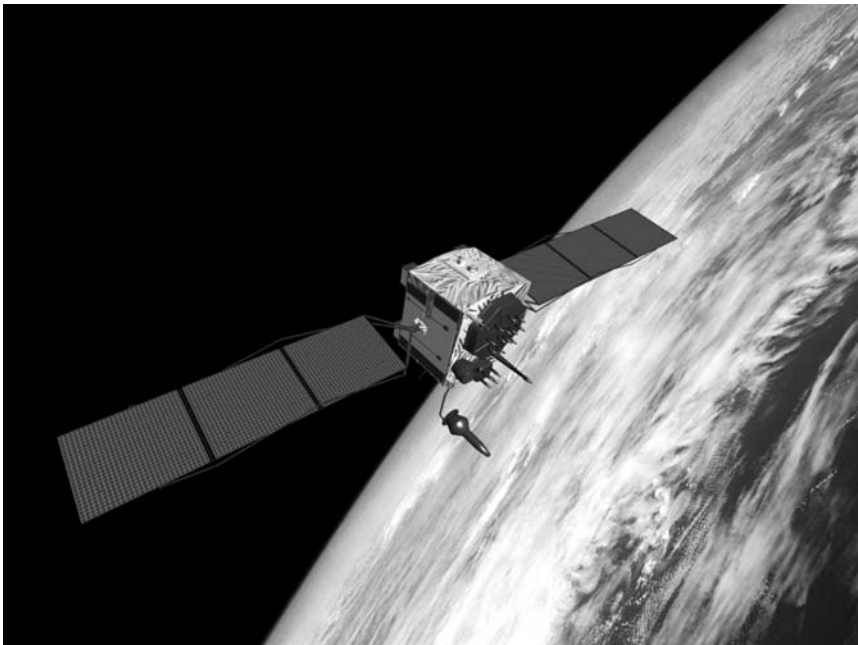


Figure 3.13 Block IIF SV (*Source: The Boeing Company. Reprinted with permission.*)

contracts and a brief planning period for the government, GPS III entered phase A development with two contracts, again to Boeing and Lockheed Martin teams. Each team completed a system requirements review in 2005. At the time of this writing, the first GPS III satellite launch was planned for fiscal year 2013.

3.3 Control Segment

The control segment (CS) is responsible for monitoring, commanding, and controlling the GPS satellite constellation. Functionally, the CS monitors the downlink L-band navigation signals, updates the navigation messages, and resolves satellite anomalies. Additionally, the CS monitors each satellite's state of health, manages tasks associated with satellite stationkeeping maneuvers and battery recharging, and commands the satellite payloads, as required [11].

The major elements of the CS consist of the MCS, L-band monitor stations, and S-band ground antennas. The primary CS functions are performed at the MCS, under the operation of the U.S. Air Force Space Command, Second Space Operation Squadron (2SOPS), located at Schriever Air Force Base (AFB) in Colorado Springs, Colorado. It provides continuous GPS services, 24 hours per day, 7 days a week, and serve as the mission control center for GPS operations. A backup MCS, located at a contractor facility in Gaithersburg, Maryland, provides redundancy of the MCS. The major elements of the CS and their functional allocation are shown in Figure 3.14.

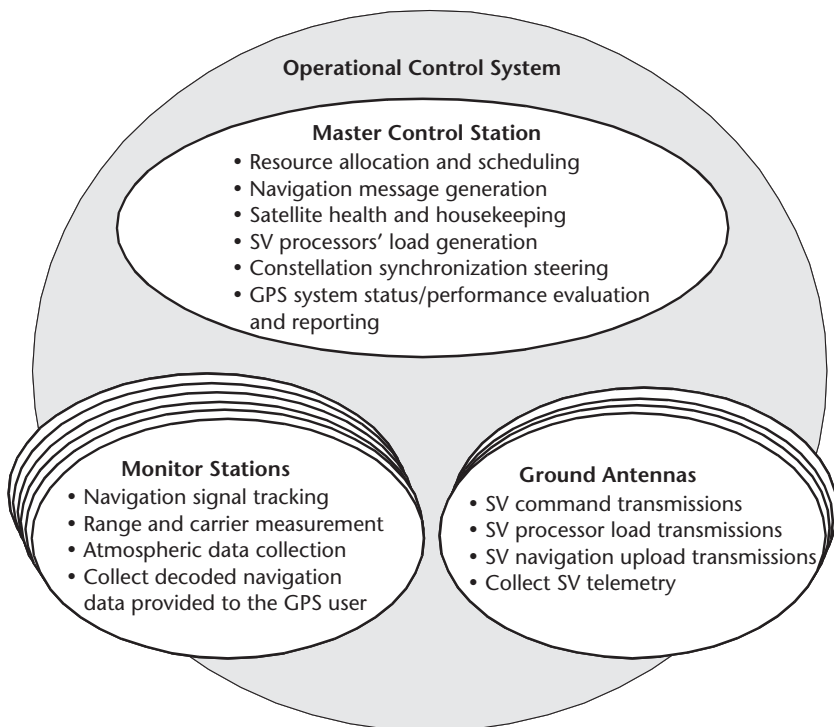


Figure 3.14 CS overview.

The 2SOPS supports all crew-action required operations of the GPS constellation, including daily uploading of navigation information to the satellites and monitoring, diagnosis, reconfiguration, and stationkeeping of all satellites in the GPS constellation. Spacecraft prelaunch, launch, and insertion operations are performed by a different ground control system under the command of the First Space Operations Squadron (1SOPS), also located at Schriever AFB. If a given SV is determined to be incapable of normal operations, the satellite commanding is transferred to 1SOPS for anomaly resolution or test monitoring.

3.3.1 Current Configuration

At the time of this writing, the CS configuration consisted of dual MCSs, six monitor stations, and four ground antennas (see Figure 3.15). The MCS data processing software, hosted on an IBM mainframe under the Multiple Virtual Storage operating system, commands and controls the CS with multiple high-definition textual displays. The monitor stations and ground antennas are unmanned and are operated remotely from the active MCS. The monitor stations' and ground antennas' data processing software, hosted on Sun workstations under the UNIX operating system, communicate with the MCS using transmission control processing/Internet processing (TCP/IP) communication protocols. The MCS also has numerous internal and external communication links. The majority of these links use the IBM's System Network Architecture communication protocol. There are plans to transition all of these links to TCP/IP.

The CS configuration is in transition. Two major upgrades are in development: the Legacy Accuracy Improvement Initiative (L-AII) and the Architecture Evolution Plan (AEP). The L-AII upgrade adds up to 14 NGA monitor stations. Therefore, there can be a total of 20 Air Force and NGA monitoring stations within the CS. These additional NGA stations will provide the CS with continuous L-band tracking coverage of the constellation. (The current six monitor station configuration can have satellite L-band coverage outages of up to 2 hours.) The AEP upgrade replaces

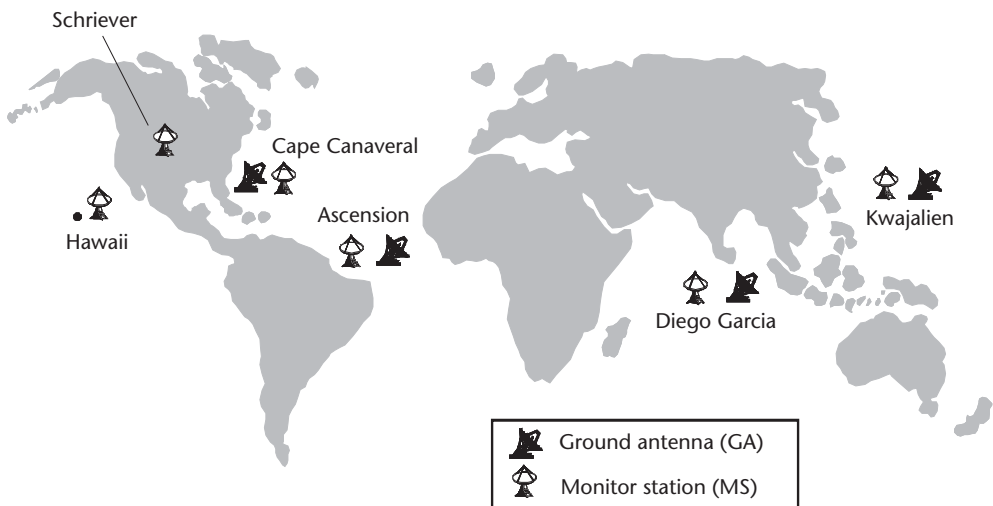


Figure 3.15 Geographic distribution of CS facilities.

the MCS legacy mainframe with a distributed Sun workstation configuration. The AEP upgrade provides an integrated suite of commercial off-the-shelf products and improved graphical user interface displays. As AEP evolves, the CS will have additional features and functionality, including support for the IIF satellites and the modernized signals (further discussion is found in Section 3.3.2).

3.3.1.1 MCS Description

The MCS provides the central command and control of the GPS constellation. Specific functions include:

- Monitoring and maintaining satellite state of health;
- Monitoring the satellite orbits;
- Estimating and predicting satellite clock and ephemeris parameters;
- Generating GPS navigation messages;
- Maintaining GPS timing service and its synchronization to UTC (USNO);
- Monitoring the navigation service integrity;
- End-around verifying and logging the navigation data delivered to the GPS user;
- Commanding satellites maneuvers to maintain the GPS orbit and repositioning due to vehicle failures.

All ground facilities necessary to support the GPS constellation are contained within the CS, as shown in Figure 3.14. The CS shares a ground antenna with the Air Force Satellite Control Network and additional monitor stations with NGA, under the L-AII and AEP upgrade. The MCS consists of data processing, control, display, and communications equipment to support these functions. The discussion here is limited to the navigation service, with no discussion related to the satellite maintenance activities.

The primary task of the MCS is to generate and distribute the navigation data message (sometimes referred to as the NAV Data message). (Details of the NAV Data message are contained in Section 4.4.) The MCS uses a sequence of steps, including collecting and processing the monitor station measurements, generating satellite ephemeris and clock estimates and predictions, and constructing and distributing the NAV Data messages. The monitor stations provide the raw pseudorange, carrier phase, and meteorological measurements that are smoothed by the MCS. A Kalman filter generates the precise satellite ephemeris and clock estimates, using these smoothed measurements. The CS filter is a linearized Kalman filter, with the ephemeris estimates linearized around a nominal reference trajectory. The reference trajectory is computed using accurate models to describe each satellite's motion. These ephemeris estimates, together with the reference trajectory, construct the precise ephemeris predictions that form the basis of the NAV Data message ephemeris parameters. Specifically, a least squares fit routine converts the predicted positions into the navigation orbital elements, in accordance with IS-GPS-200 (see Section 2.3.1). The resulting orbital elements are uploaded into the satellite's navigation payload memory and transmitted to the GPS user.

Fundamentally, GPS navigation accuracy is derived from a coherent time scale, known as GPS system time, with one of the critical components being the satellite's AFS, which provides the stable reference for the satellite clock. As discussed earlier, each satellite carries multiple AFSs. The MCS commands the satellite AFSs, monitors their performance, and maintains estimates of satellite clock bias, drift, and drift rate (for rubidium only) to support the generation of clock corrections for the NAV Data message. As stated in Section 2.6, GPS system time is defined relative to an ensemble of all active SV and MS AFSs. The ensemble or composite AFS improves GPS time stability and minimizes its dependency on any single AFS failure in defining such a coherent time scale.

Another important task of the MCS is to monitor the integrity of the navigation service. Throughout the entire data flow from MCS to satellite and back, the MCS ensures that all NAV Data message parameters are uploaded and transmitted correctly. The MCS maintains a complete memory image of the NAV Data message and compares each downlink message (received from its monitor stations) against the expected message. Significant differences between the downlink versus expected navigation message result in an alert and corrective action by 2SOPS. Along with navigation bit errors, the MCS monitors the L-band ranging data for consistency across satellites and across monitor stations. When an inconsistency is observed across satellites or monitor stations, the MCS generates an L-band alert within 60 seconds of detection [12].

The CS depends on several external data sources for coordination with the UTC (USNO) absolute time scale, precise monitor station coordinates, and Earth-orientation parameters. NGA and USNO provide the CS with such external data.

3.3.1.2 Monitor Station Description

To perform the navigation tracking function, the CS has a dedicated, globally distributed, L-band monitor station network. At the time of this writing, the CS network consisted of six Air Force monitor stations: Ascension Island, Diego Garcia, Kwajalein, Hawaii, Colorado Springs, and Cape Canaveral. These stations are located near the equator to maximize L-band coverage and are shown in Figure 3.16.

Each monitor station operates under the control of the MCS and consists of the equipment and computer programs necessary to collect satellite-ranging data, satellite status data, and local meteorological data. This data is forwarded to the MCS for processing. Specifically, a monitor station consists of a single dual-frequency receiver, dual cesium AFSs, meteorological sensors, and local workstations and communication equipment. Each receiver's antenna element consists of a conical ground plane with annular chokes at the base to produce a 14-dB multipath-to-direct signal rejection ratio for signal paths above 15° elevation. (An in-depth discussion on multipath is contained in Section 6.2.) The HP5071 cesium AFSs provide a 5-MHz reference to the receiver. Continuous-phase measurements between the AFSs are provided to the MCS for independent monitoring of the active atomic clock and for support of AFS switchovers. The MCS maintains a coherent monitor station time scale. At AFS switchovers, the MCS provides the phase and frequency difference estimates (between AFSs) to the CS Kalman filter to minimize any time

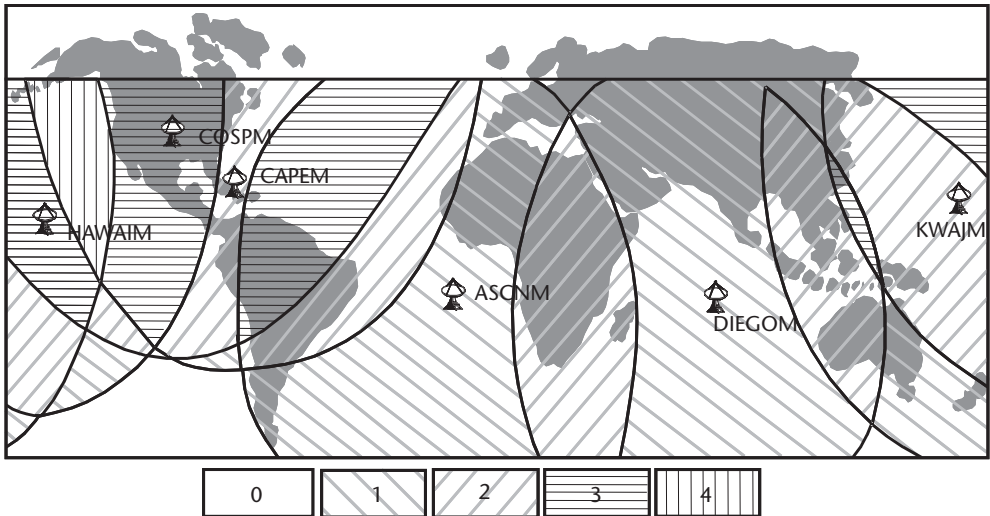


Figure 3.16 CS monitor station coverage.

scale disruptions. Meteorological sensors provide surface pressure, temperature, and dew point measurements to the CS Kalman filter to model the troposphere delay. However, these meteorological sensors are in disrepair, and their measurements have been replaced by monthly tabular data [13]. The local workstations provide commands and data collection between the monitor station and the MCS.

The Air Force monitor stations use a 12-channel, survey-grade, all-in-view receiver. These receivers, developed by Allen Osbourne Associates (AOA), are based on proven Jet Propulsion Laboratory (JPL) Turbo Rogue technology. The AOA receiver is designed with complete independence of the L1 and L2 tracking loops, with each tracking loop commanded by the MCS under various track acquisition strategies. With such a design, the overall receiver tracking performance can be maintained, even when tracking abnormal satellites (e.g., nonstandard code or satellite initialization, which require additional acquisition processing). These all-digital receivers have no detectable interchannel bias errors. (An earlier CS receiver required external interchannel bias compensation due to its analog design with separate correlation and data processing cards. Interchannel bias is a time-delay difference incurred when processing a common satellite signal through different hardware and data processing paths in a receiver.)

The CS receivers differ from normal receivers in several areas. First, these receivers require external commands for acquisition. Although most user equipment is only designed to acquire and track GPS signals that are in compliance with applicable specifications, the CS receiver needs to track signals even when they are not in compliance. The external commands allow the CS receiver to acquire and track abnormal signals from unhealthy satellites. Second, all measurements are time tagged to the satellite X1 epoch (see Section 4.3.1.1 for further details on the X1 epoch), whereas a typical user receiver time tags range measurements relative to the receiver's X1 epoch. Synchronizing measurements relative to the satellite's X1 epochs facilitates the MCS's processing of data from the entire distributed CS L-band Monitor Station Network. The CS receivers provide the MCS with 1.5-

second pseudorange and accumulated delta range measurements (also known as P-code and carrier phase measurements, respectively). Third, the MCS receives all of the raw demodulated navigation bits from each monitor station (without processing of the Hamming code used for error detection) so that problems in the NAV Data message can be observed. The returned NAV Data message is compared bit by bit against expected values to provide a complete system-level verification of the MCS-ground antenna-satellite-monitor station data path. Additionally, the CS receivers provide the MCS with various internal signal indicators, such as time of lock of the tracking loops and internally measured signal-to-noise ratio (SNR). This additional data is used by the MCS to discard questionable measurements from the CS Kalman filter. As noted earlier, the CS maintains the monitor station time scale to accommodate station time changes, failures, and reinitialization of the station equipment. The Air Force monitor station coverage of the GPS satellites is shown in Figure 3.16, with the grayscale code denoting the number of monitor stations visible to a satellite [14]. Satellite coverage varies from zero in the region west of South America to as many as three in the continental United States.

3.3.1.3 Ground Uplink Antenna Description

To perform the satellite commanding and data transmission function, the CS includes a dedicated, globally distributed, ground antenna network. Currently, the CS network, colocated with the Air Force monitor stations, consists of Ascension Island, Diego Garcia, Kwajalein, and Cape Canaveral. The Cape Canaveral facility also serves as part of the prelaunch compatibility station supporting prelaunch satellite compatibility testing. Additionally, one automated remote tracking station ground antenna located in Colorado, from the Air Force Satellite Control Network, serves as a GPS ground antenna. These ground antennas provide the TT&C interface between the CS and the space segment for uploading the navigation data.

These ground antennas are full-duplex, S-band communication facilities that have dedicated command and control sessions with a single SV at a time. Under MCS control, multiple simultaneous satellite contacts can be performed. Each ground antenna consists of the equipment and computer programs necessary to transmit commands, navigation data uploads, and payload control data received from the MCS to the satellites and to receive satellite telemetry data that is forwarded to the MCS. All CS ground antennas are dual-threaded for system redundancy and integrity. The CS ground antennas have been recently upgraded to support S-band ranging. The S-band ranging provides the CS with the capability to perform satellite early orbit and anomaly resolution support. The ground antenna coverage of the GPS satellites is shown in Figure 3.17, with the grayscale code denoting the number of ground antennas visible to a satellite [14].

3.3.1.4 MCS Data Processing

MCS Measurement Processing

To support the MCS estimation and prediction function, the CS continuously tracks the L1 and L2 P(Y) codes. At track acquisition, the L1 C/A code is sampled during the handover to P(Y) code to ensure that it is being broadcast (however, the

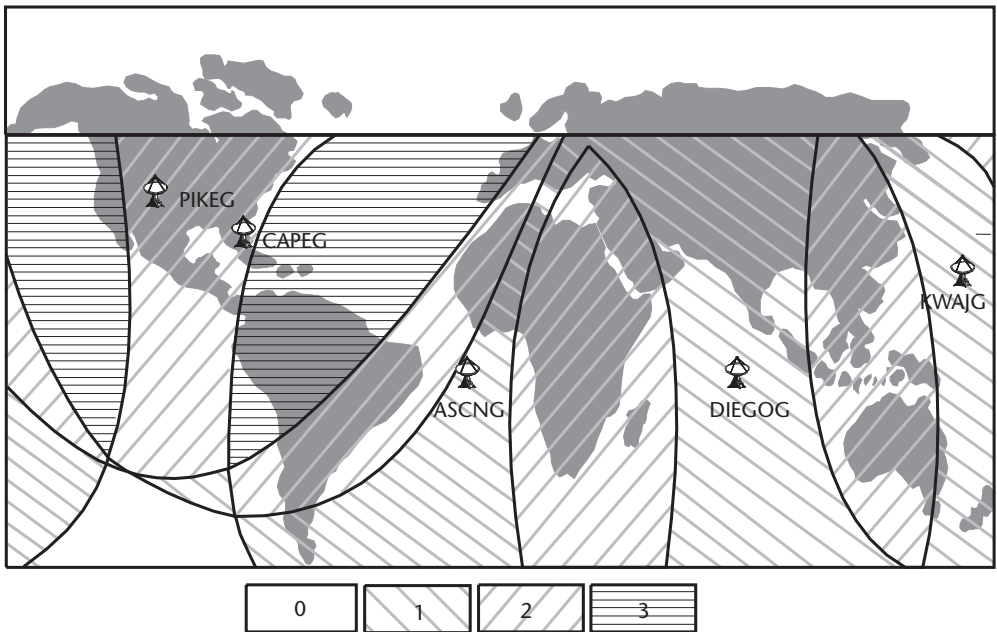


Figure 3.17 CS ground antenna coverage.

CS does not continuously track the L1 C/A code). The raw 1.5-second L1 and L2 pseudorange and carrier phase (also known as accumulated delta range) measurements are converted at the MCS into 15-minute smoothed measurements. The smoothing process uses the carrier phase measurements to smooth the pseudorange data to reduce the measurement noise. The process provides smoothed pseudorange and sampled carrier phase measurements for use by the CS Kalman filter.

The smoothing process consists of data editing to remove outliers and cycle slips, converting raw dual-frequency measurements to ionosphere-free observables, and generating smoothed measurements once a sufficient number of validated measurements are available. Figure 3.18 shows a representative data smoothing interval consisting of 600 pseudorange and carrier phase observations, with 595 observations used to form a smoothed pseudorange minus carrier phase offset and the 5 remaining observations used to form a carrier phase polynomial.

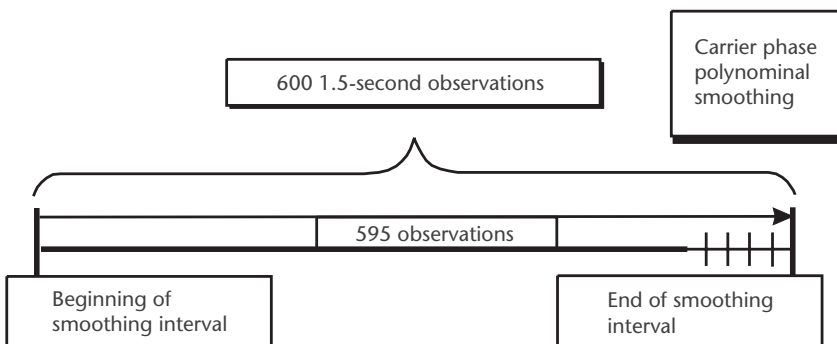


Figure 3.18 Representative MCS data-smoothing interval.

The CS data editing limit checks the pseudoranges and performs third-difference tests on the raw L1 and L2 observables. The third-difference test compares consecutive sequences of L1 and L2 observables against thresholds. If the third-difference test exceeds these thresholds, then those observables are discarded for subsequent use in that interval. Such data editing protects the CS Kalman filter from questionable measurements. Ionosphere-corrected, L1 pseudorange, and phase measurements, ρ_c and ϕ_c , respectively, are computed using the standard ionosphere correction (see Section 7.2.4.1):

$$\begin{aligned}\rho_c &= \rho_1 - \frac{1}{(1-\alpha)} \cdot (\rho_1 - \rho_2) \\ \phi_c &= \phi_1 + \frac{1}{(1-\alpha)} \cdot (\phi_1 - \phi_2)\end{aligned}\quad (3.1)$$

where $\alpha = (154/120)^2$, and ρ_i and ϕ_i for $i = 1, 2$ are the validated L1 and L2 pseudorange and phase measurements, respectively.

Ionosphere-corrected pseudorange and carrier-phase measurements are related by a constant offset. By exploiting this fact, a smoothed pseudorange measurement, $\bar{\rho}_c$, is formed from a carrier phase as follows:

$$\bar{\rho}_c = \phi_c + B \quad (3.2)$$

where B is an unknown constant computed by averaging the L1 ionosphere-corrected pseudorange and carrier-phase measurement, ρ_c and ϕ_c , differences

$$B = \sum (\rho_c(z_j) - \phi_c(z_j)) \quad (3.3)$$

over all validated measurements in the smoothing interval. The CS pioneered such carrier-aided smoothing of pseudoranges in the early 1980s.

The CS Kalman filter performs measurement updates every 15 minutes based on its uniform GPS time scale (i.e., GPS system time). The smoothing process generates second-order pseudorange and carrier-phase measurement polynomials in the neighborhood of these Kalman update times. A phase measurement polynomial, consisting of bias, drift, and drift rate, $\hat{\mathbf{X}}_c$, is formed using a least-squares fit of the last five phase measurements in the smoothing interval, $\bar{\Phi}_c$:

$$\hat{\mathbf{X}}_c = (\mathbf{A}^T \mathbf{W} \mathbf{A})^{-1} \cdot \mathbf{A}^T \mathbf{W} \bar{\Phi}_c \quad (3.4)$$

where

$$\mathbf{A} = \begin{bmatrix} 1 & -2\tau & 4\tau^2 \\ 1 & -\tau & \tau^2 \\ 1 & 0 & 0 \\ 1 & \tau & \tau^2 \\ 1 & 2\tau & 4\tau^2 \end{bmatrix}, \quad \bar{\Phi}_c = \begin{bmatrix} \phi_c(z_{-2}) \\ \phi_c(z_{-1}) \\ \phi_c(z_0) \\ \phi_c(z_1) \\ \phi_c(z_2) \end{bmatrix} \quad (3.5)$$

where τ equals 1.5 seconds and $\{z_i$, for $i = -2, -1, 0, 1, 2\}$ denotes the time tags associated with the last five phase measurements in the interval. The weighting matrix, \mathbf{W} in (3.4), is diagonal with weights derived from the receiver's reported SNR value. The pseudorange measurement polynomial, $\hat{\mathbf{X}}_p$, is formed using the constant offset in (3.3) as follows:

$$\hat{\mathbf{X}}_p = \hat{\mathbf{X}}_c + \begin{bmatrix} B \\ 0 \\ 0 \end{bmatrix} \quad (3.6)$$

These smoothed pseudorange and phase measurements, in (3.6) and (3.4) respectively, are interpolated by the CS Kalman filter to a common GPS time scale, using the satellite clock estimates.

MCS Ephemeris and Clock Processing

The MCS ephemeris and clock processing software continuously estimates the satellite ephemeris and clock states, using a Kalman filter with 15-minute updates based on the smoothed measurements described earlier. The MCS ephemeris and clock estimates are used to predict the satellite's position and clock at future times to support the generation of the NAV Data message.

The MCS ephemeris and clock processing is decomposed into two components: offline processing for generating reference trajectories, inertial-to-geodetic coordinate transformations, and Sun/Moon ephemeris, and real-time processing associated with maintaining the CS Kalman filter estimates. The MCS offline processing depends on highly accurate models. The CS reference trajectory force models [15, 16] include the WGS-84 Earth gravitational harmonics (truncated to degree 8 and order 8), the satellite-unique solar radiation models, the solar and lunar gravitational effects (derived from the JPL Solar Ephemeris, DE200), and the solar and lunar solid tidal effects (second-degree Legendre polynomials). The magnitude of these various forces and their corresponding effect on the GPS orbits has been analyzed and is summarized in Table 3.5 [17].

The differences on the left- and right-hand sides of Table 3.5 quantify the positional error due to that component on the ephemeris trajectory and orbit determination, respectively. Since the equations of motion describing GPS orbits are nonlinear, the CS linearizes the ephemeris states around a nominal reference trajectory [18, 19]. To support ephemeris predictions, these ephemeris estimates are maintained relative to the reference trajectory's epoch states and the trajectory partials (relative to the epoch) used to propagate to current or future times.

The CS Kalman filter tracks the satellite ephemeris in ECI coordinates and transforms the satellite positions into ECEF coordinates using a series of rotation matrices (as described in Section 2.2). These ECI-to-ECEF coordinate rotation matrices account for luni-solar and planetary precession, nutation, Earth rotation, polar motion, and UT1-UTC effects. (Polar motion and UT1-UTC Earth orientation predictions are provided weekly to the CS by the NGA.)

The CS Kalman state estimate consists of three ECI positions and velocities, two solar pressures, and up to three clock states for each satellite, along with a tropospheric wet height and two clock states for each monitor station. The two solar

Table 3.5 Acceleration Forces Perturbing Satellite Orbit

Perturbing Acceleration	RMS Orbit Differences over 3 Days (m)				RMS Orbit Determination (m)			
	Radial	Along Track	Cross Track	Total	Radial	Along Track	Cross Track	Total
Earth oblateness (C_{20})	1,341	36,788	18,120	41,030	1,147	1,421	6,841	7,054
Moon gravitation	231	3,540	1,079	3,708	87	126	480	504
Sun gravitation	83	1,755	431	1,809	30	13	6	33
C_{22}, S_{22}	80	498	10	504	3	3	4	5
$C_{nm}, S_{nm} (n,m = 3..8)$	11	204	10	204	4	13	5	15
$C_{nm}, S_{nm} (n,m = 4..8)$	2	41	1	41	1	2	1	2
$C_{nm}, S_{nm} (n,m = 5..8)$	1	8	0	8	0	0	0	0
Solar radiation pressure	90	258	4	273	0	0	0	0.001

pressure states consist of a scaling parameter to the a priori solar pressure model and a Y-body axis acceleration. The Kalman filter clock states include a bias, drift, and draft rate (for Rubidium only). To avoid numerical instability, the CS Kalman filter is formulated in U-D factored form, where the state covariance (e.g., \mathbf{P}) is maintained as:

$$\mathbf{P} = \mathbf{U} \cdot \mathbf{D} \cdot \mathbf{U}^T \quad (3.7)$$

with \mathbf{U} and \mathbf{D} being upper triangular and diagonal matrices, respectively [19]. The U-D filter improves the numerical dynamic range of the CS filter estimates, whose time constants vary from several hours to several weeks. The CS Kalman time update has the form:

$$\tilde{\mathbf{U}}(t_{k+1})\tilde{\mathbf{D}}(t_{k+1})\tilde{\mathbf{U}}(t_{k+1})^T = \left[\mathbf{B}(t_k) | \hat{\mathbf{U}}(t_k) \right] \begin{bmatrix} \mathbf{Q}(t_k) \\ \hat{\mathbf{D}}(t_k) \end{bmatrix} \begin{bmatrix} \mathbf{B}(t_k)^T \\ \hat{\mathbf{U}}(t_k)^T \end{bmatrix} \quad (3.8)$$

where $\hat{\mathbf{U}}(\cdot)$, $\hat{\mathbf{D}}(\cdot)$ and $\tilde{\mathbf{U}}(\cdot)$, $\tilde{\mathbf{D}}(\cdot)$ denote the a priori and a posteriori covariance factors, respectively; $\mathbf{Q}(\cdot)$ denotes the state process noise matrix; and $\mathbf{B}(\cdot)$ denotes the matrix that maps the process noise to the appropriate state domain. The CS process noises include the satellite and ground station clocks, troposphere-wet height, solar pressure, and ephemeris velocity (with the latter being in radial, along-track, and cross-track coordinates [20]). Periodically, the 2SOPS retunes the satellite and ground station clock process noises, using on-orbit GPS Allan and Hadamard clock characterization, as provided by the Naval Research Laboratory [21, 22]. The CS Kalman filter performs scalar measurement updates, with a statistically consistent test to detect outliers (based on the measurement residuals or innovation process [18]). The CS measurement model includes a clock polynomial model (up to second order), the Hopfield/Black troposphere model [23, 24], the IERS station tide displacement model (vertical component only), and periodic relativity and satellite phase center corrections.

Since a pseudorange measurement is simply the signal transit time between the transmitting satellite and the receiving monitor station, the CS Kalman filter can

estimate both the ephemeris and clock errors. However, any error common to all of the clocks remains unobservable. Essentially, given a system of n clocks, there are only equivalently $n - 1$ separable clock observables, leaving one unobservable state. An early CS Kalman filter design avoided this unobservability by artificially forcing a single monitor station clock as the *master* and referencing all CS clock estimates to that station. Based on the theory of composite clocks, developed in [25], the CS Kalman filter was upgraded to exploit this unobservability and established GPS system time as the ensemble of all active AFSs. At each measurement update, the composite clock reduces the clock estimate uncertainties [20]. Also with the composite clock, GPS time is steered to UTC (USNO) absolute time scale for consistency with other timing services. Common view of the satellites from multiple monitor stations is critical to the estimation process. This closure of the time-transfer function provides the global time scale synchronization necessary to achieve submeter estimation performance. Given such advantages of the composite clock, the International GPS Service (IGS) has recently transitioned its products to IGS system time along the lines of the composite clocks [26].

The CS Kalman filter has several unique features. First, the CS Kalman filter is decomposed into smaller minifilters, known as partitions. The CS partitioned Kalman filter was required due to computational limitations in the 1980s. In a single partition, the Kalman filter estimates up to six satellites and all ground states, with logic across partitions to coordinate the alignment of the redundant ground estimates. Second, the CS Kalman filter has constant state estimates (i.e., filter states with zero covariance). (This feature is used in the cesium and rubidium AFS models, which are linear and quadratic polynomials, respectively). Classically, Kalman theory requires the state covariance to be positive-definite. However, given the U-D time update in (3.8) and its associated Gram-Schmidt factorization [19], the a posteriori covariance factors, $\tilde{\mathbf{U}}(\cdot)$, $\tilde{\mathbf{D}}(\cdot)$, are constructed to be positive semidefinite with selected states having zero covariance. Third, the CS Kalman filter supports Kalman backups. The CS Kalman backup consists of retrieving prior filter states and covariances (up to the past 24 hours) and reprocessing the smoothed measurement under different filter configurations. This backup capability is critical to 2SOPS for managing satellite, ground station, or operator-induced abnormalities. The CS Kalman filter has various controls available to 2SOPS to manage special events, including AFS runoffs, autonomous satellite jet firings, AFS reinitializations and switchovers of AFSs, reference trajectories, and Earth orientation parameter changes. The CS Kalman filter has been continuously running since the early 1980s with no filter restarts.

MCS Upload Message Formulation

The MCS upload navigation messages are generated by a sequence of steps. First, the CS generates predicted ECEF satellite antenna phase center positions, denoted as $[\tilde{\mathbf{r}}_{sa}(\cdot | t_k)]_E$, using the most recent Kalman filter estimate at time, t_k . Next, the CS performs a least squares fit of these predicted positions using the NAV Data message ephemeris parameters. The least squares fits are over either 4-hour or 6-hour time intervals, also known as a subframe. (Note that the subframe fitting intervals are longer for the extended operation uploads.) The 15 orbital elements (see Section 2.3.1, Table 2.2) can be expressed in vector form as

$$\mathbf{X}(t_{oe}) \equiv \left[\sqrt{a}, e, M_0, \omega, \Omega_0, i_0, \dot{\Omega}, \dot{i}, \Delta n, C_{uc}, C_{us}, C_{ic}, C_{is}, C_{rc}, C_{rs} \right]^T \quad (3.9)$$

with an associated ephemeris reference time, t_{oe} , and are generated using a nonlinear weighted least squares fit.

For a given subframe, the orbital elements, $\mathbf{X}(t_{oe})$, are chosen to minimize the performance objective:

$$\sum_{\ell} \left\{ \left(\left[\bar{r}_{sa}(t_{\ell} | t_k) \right]_E - g_{epb}(t_{\ell}, \mathbf{X}(t_{oe})) \right)^T \mathbf{W}(t_{\ell}) \right\} \quad (3.10)$$

where $g_{epb}(\cdot)$ is a nonlinear function mapping the orbital elements, $\mathbf{X}(t_{oe})$, to an ECEF satellite antenna phase center position (see Section 2.3.1, Table 2.3) and $\mathbf{W}(\cdot)$ is a weighting matrix.

As defined in (3.10), all position vectors and associated weighting matrices are in ECEF coordinates. Since the CS error budget is defined relative to the user range error (see Section 7.2), the weighting matrix is resolved into radial, along-track, and cross-track (RAC) coordinates, with the radial given the largest weight. The weighting matrix of (3.10) has the form:

$$\mathbf{W}(t_{\ell}) = \mathbf{M}_{E \leftarrow RAC}(t_{\ell}) \cdot \mathbf{W}_{RAC}(t_{\ell}) \cdot \mathbf{M}_{E \leftarrow RAC}(t_{\ell})^T \quad (3.11)$$

where $\mathbf{M}_{E \leftarrow RAC}(\cdot)$ is a coordinate transformation from RAC to ECEF coordinates, and \mathbf{W}_{RAC} is a diagonal RAC weighting matrix.

For the orbital elements in (3.9), the performance objective in (3.10) can become ill conditioned for small eccentricity, e . An alternative orbital set is introduced to remove such ill conditioning; specifically, three auxiliary elements defined as follows:

$$\alpha = e \cos \omega, \quad \beta = e \sin \omega, \quad \gamma = M_0 + \omega \quad (3.12)$$

Thus, the objective function in (3.10) is minimized relative to the alternative orbital elements, $\bar{\mathbf{X}}(\cdot)$ having the form:

$$\bar{\mathbf{X}}(t_{oe}) \equiv \left[\sqrt{a}, \alpha, \beta, \gamma, \Omega_0, i_0, \dot{\Omega}, \dot{i}, \Delta n, C_{uc}, C_{us}, C_{ic}, C_{is}, C_{rc}, C_{rs} \right]^T \quad (3.13)$$

The three orbital elements (e, M_0, ω) are related to the auxiliary elements, (α, β, γ) by the inverse mapping

$$e = \sqrt{\alpha^2 + \beta^2}, \omega = \tan^{-1}(\beta/\alpha), M_0 = \gamma - \omega \quad (3.14)$$

The advantage of minimizing (3.10) with respect to $\bar{\mathbf{X}}(\cdot)$ in (3.13) versus $\mathbf{X}(\cdot)$ in (3.9) is that the auxiliary orbital elements are well defined for small eccentricity.

The minimization problem in (3.10) and (3.14) is simplified by linearizing $g_{epb}(\cdot)$ about a nominal orbital element set, denoted by $\bar{\mathbf{X}}_{nom}(t_{oe})$ such that

$$g_{epb}(t_\ell, \bar{\mathbf{X}}(t_{oe})) = g_{epb}(t_\ell, \bar{\mathbf{X}}_{nom}(t_{oe})) + \left. \frac{\partial g_{epb}(t_\ell, \lambda)}{\partial \lambda} \right|_\lambda = \bar{\mathbf{X}}_{nom}(t_{oe}) \cdot (\bar{\mathbf{X}}(t_{oe}) - \bar{\mathbf{X}}_{nom}(t_{oe})) \quad (3.15)$$

and then (3.10) becomes equivalently

$$\sum_\ell \left\{ \left(\left[\Delta \bar{r}_{sa}(t_\ell | t_k) \right]_E - \mathbf{P}(t_\ell, \bar{\mathbf{X}}_{nom}(t_{oe})) \cdot \Delta \bar{\mathbf{X}}(t_{oe}) \right)^T \cdot \mathbf{W}(t_\ell) \cdot \left(\left[\Delta \bar{r}_{sa}(t_\ell | t_k) \right]_E - \mathbf{P}(t_\ell, \bar{\mathbf{X}}_{nom}(t_{oe})) \cdot \Delta \bar{\mathbf{X}}(t_{oe}) \right) \right\} \quad (3.16)$$

where

$$\left[\Delta \bar{r}_{sa}(t_\ell | t_k) \right]_E = \left[\bar{r}_{sa}(t_\ell | t_k) \right]_E - g_{epb}(t_\ell, \mathbf{X}_{nom}(t_{oe})) \quad (3.17)$$

$$\mathbf{P}(t_\ell, \mathbf{X}_{nom}(t_{oe})) = \left. \frac{\partial g_{epb}(t_\ell, \lambda)}{\partial \lambda} \right|_\lambda = \bar{\mathbf{X}}_{nom}(t_{oe}) \quad (3.18)$$

$$\Delta \bar{\mathbf{X}}(t_{oe}) = \bar{\mathbf{X}}(t_{oe}) - \bar{\mathbf{X}}_{nom}(t_{oe}) \quad (3.19)$$

Following classical least square techniques (see description in Appendix A) applied to the performance objective in (3.16) yields

$$\begin{aligned} & \sum_t \left\{ \mathbf{P}(t_\ell, \bar{\mathbf{X}}_{nom}(t_{oe}))^T \mathbf{W}(t_\ell) \mathbf{P}(t_\ell, \bar{\mathbf{X}}_{nom}(t_{oe})) \right\} \Delta \bar{\mathbf{X}}(t_{oe}) \\ & = \sum_\ell \left\{ \mathbf{P}(t_\ell, \bar{\mathbf{X}}_{nom}(t_{oe}))^T \mathbf{W}(t_\ell) \left[\Delta \bar{r}_{sa}(t_\ell | t_k) \right]_E \right\} \end{aligned} \quad (3.20)$$

where the solution, $\Delta \bar{\mathbf{X}}(t_{oe})$, is referred to as the differential correction. Since $g_{epb}(\cdot)$ is nonlinear, the optimal orbital elements in (3.16) are obtained by successive iteration: first, a nominal orbital vector, $\bar{\mathbf{X}}_{nom}(t_{oe})$, followed by a series of the differential correction, $\Delta \bar{\mathbf{X}}(t_{oe})$ using (3.20), until the differential correction converges to zero. Following a similar approach, the almanac and clock navigation parameters are also generated. These resulting orbital elements, $\bar{\mathbf{X}}(\cdot)$, are then scaled and truncated in compliance with the NAV Data message format. Note, these orbital elements, $\bar{\mathbf{X}}(\cdot)$, are quasi-Keplerian and represent a local fit of the satellite ECEF trajectory, and they are not acceptable for overall orbit characterization.

Representative curve fit errors, associated with the NAV Data message generation described earlier, are shown in Figure 3.19. For 4-hour utilization intervals, three performance metrics are depicted: RMS URE, the maximum URE, and the root sum squared (RSS) position errors. For the June–July 2000 period and across all satellites, the constellation RMS-URE, Max-URE, and Max-RSS errors were 8.72, 14.7, and 52.9 cm (RMS), respectively, with along-track component being the dominant error.

MCS Upload Message Dissemination

Nominally, each satellite's NAV Data message is uploaded at least once per day. Before each new upload transmission, the NAV Data message is verified to be in

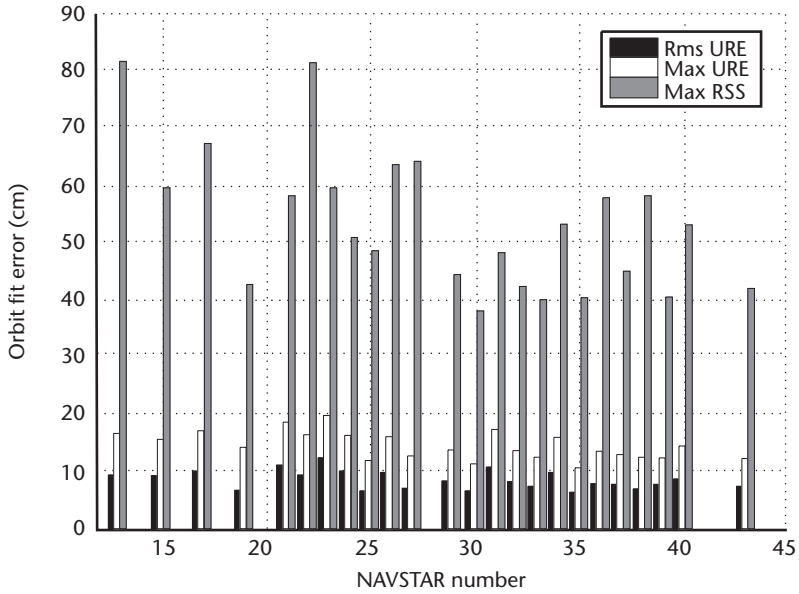


Figure 3.19 MCS upload message fit errors.

compliance with IS-GPS-200, with navigation bits populating the subframes. Additionally, the MCS-ground antenna-satellite uploads are checked, after the navigation data is locked into the satellite’s memory and prior to authorizing the L-band transmission. Error protection codes exist along the entire path of navigation service for integrity. The satellite upload communication protocol is enforced to assure proper and error-free data content onboard the satellite before its use is authorized.

The NAV Data is based on predictions of the CS Kalman filter estimates, which degrade with age of data. The 2SOPS monitors the navigation accuracy and performs contingency uploads when the accuracy exceeds specific thresholds. Unfortunately, the dissemination of the NAV Data message is a tradeoff of upload frequency to navigation accuracy. Various upload strategies have been evaluated to minimize upload frequency while maintaining an acceptable navigation service [6, 27]. Figure 3.20 shows the basis tradeoff curve: an increase in upload frequency reduces the prediction age of data and thus improves the signal-in-space URE (see Section 7.2). GPS navigation accuracy depends on many factors, including performance of the satellite AFSs, the number and placement of the monitor stations, measurement errors, ephemeris modeling, and filter tuning.

3.3.2 CS Planned Upgrades

Over the next several years, the CS will field two major upgrades: the L-AII and the AEP. The L-AII upgrade modifies the existing MCS mainframe implementation to support additional monitor stations and satellites in a partitioned Kalman filter. Since the 1980s, the MCS has used a partitioned Kalman filter consisting of up to six satellites and up to six monitor stations per partition. This partition filter design was due to computational limitations and hindered CS navigation accuracy. The L-AII upgrade will enable the MCS to support up to 20 monitor stations and up to 32 satellites in a partition. (Note: The CS Kalman filter will maintain the partitioning and

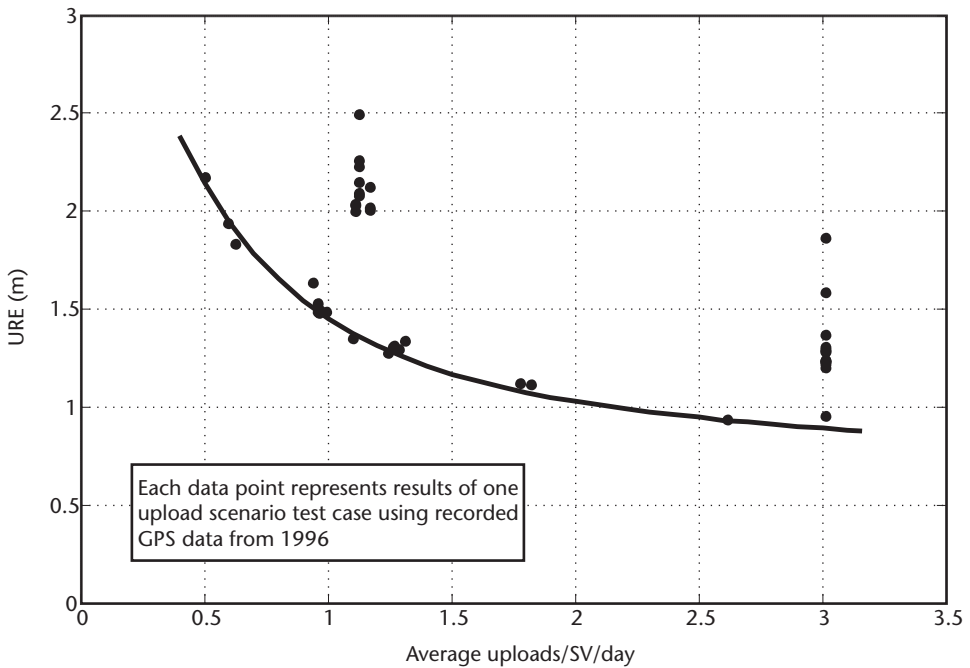


Figure 3.20 MCS uploads versus navigation accuracy. (From: [27]. 1997 IONS. Reprinted with permission.)

backup capabilities to support satellite abnormalities.) NGA will provide additional monitoring stations for the MCS with 15-minute smoothed and 1.5-second raw pseudorange and carrier phase measurements from Ashtech geodetic-quality receivers. These smoothed and raw measurements will be used in the CS Kalman filter and L-band monitor [12] processing, respectively. Once operational, the CS Kalman filter zero-age-of-data URE will be reduced approximately by one-half [6, 28] and the L-band monitor visibility coverage will be increased from 1.5 monitor stations/satellite to 3 to 4 monitor stations/satellite. The combined Air Force and NGA monitor station network is shown in Figure 3.21.

The L-AII upgrade includes several model improvements to the MCS processing. The existing and planned model updates are summarized in Table 3.6.

Various U.S. government agencies, research laboratories, and the international GPS community have developed improved GPS models over the past 20 years. These L-AII model updates of geopotential, station-tide displacement, and Earth orientation parameter enable the MCS processing to be compliant with the conventions of the IERS [29]. The recently developed JPL solar pressure model improves the satellite ephemeris dynamic modeling with the inclusion of Y-axis, β -dependent force, where β is the angle between the Sun-Earth line and the satellite orbital plane. The Neill/Saastamoinen model improves tropospheric modeling at low elevations.

The AEP upgrade replaces the MCS mainframe with a distributed Sun workstation configuration. The AEP upgrade extends beyond the L-AII upgrade to include an integrated suite of commercial off-the-shelf products and an improved graphical user interface. The AEP update is an object-oriented software design using TCP/IP communication protocols across workstations connected by a 1-GB Ethernet local



Figure 3.21 Combined Air Force and NGA monitor station network.

Table 3.6 Existing and Planned Model Upgrades

Model	Existing MCS Capability [15, 20]	Planned MCS Upgrade
Geopotential model	WGS84 (8 × 8) gravitational harmonics	EGM 96 (12 × 12) gravitational harmonics [29]
Station tide displacement	Solid tide displacement accounting for lunar and solar vertical component only	IERS 2003, including vertical and horizontal components [29]
Earth orientation parameters	No zonal or diurnal/semidiurnal tidal compensation	Restoration of zonal tides and application of diurnal/semidiurnal tidal corrections [29]
Solar radiation pressure model	Rockwell Rock42 model for Block II/IIA and Lockheed Martin Lookup model for IIR	JPL empirically derived solar pressure model [30]
Troposphere model	Hopfield/Black model	Neill/Saastamoinen model [31, 32]

area network (LAN). The AEP distributed architecture maintains the MCS operational data in an Oracle database (with a standby failover strategy).

The AEP upgrade provides the infrastructure for incremental MCS improvements, including support for the IIF satellites and the modernized signals (see Sections 3.2.3.7 and 4.5, respectively). Regarding the modernized signals, an alternative NAV Data message representation will be deployed with additional parameters and reduced quantization errors. Representative curve fit errors associated with the modernized NAV Data message are shown in Figure 3.22. For 3-hour utilization intervals, three performance metrics are depicted: RMS URE, the maximum URE, and the RSS position errors. For the June–July 2000 period and across all satellites, the constellation RMS-URE, Max-URE, and Max-RSS errors were 0.543, 0.943, and 3.56 cm (RMS), respectively. A comparison with the results of Figure 3.19 shows that the modernized signals curve fit errors will be significantly reduced.

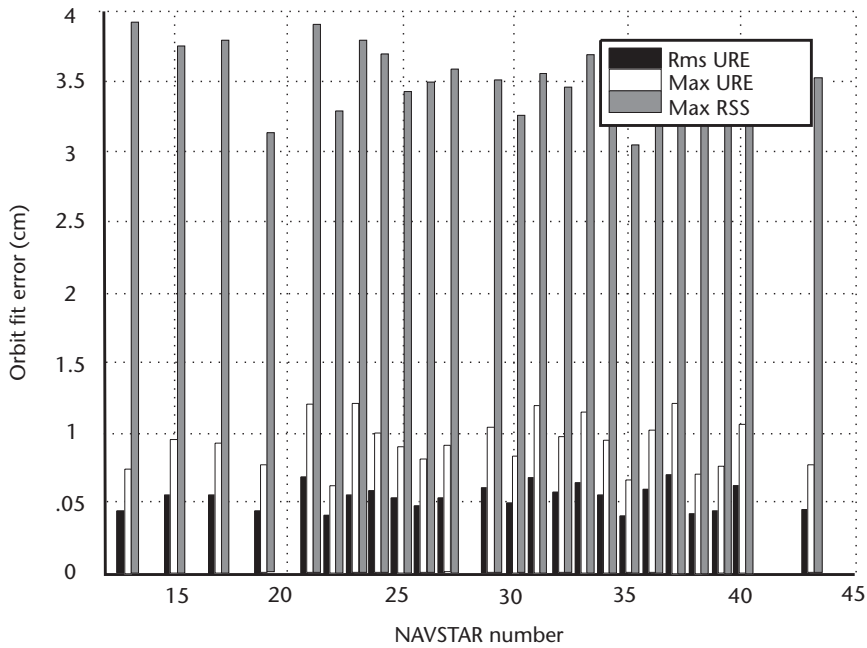


Figure 3.22 Modernized signal message fit errors.

3.4 User Segment

The user receiving equipment, typically referred to as a GPS receiver, processes the L-band signals transmitted from the satellites to determine PVT. Technology trends in component miniaturization and large-scale manufacturing have led to a proliferation of low-cost GPS receiver components. GPS receivers are embedded in many of the items we use in our daily lives. These items include cellular telephones, PDAs, and automobiles. This is in contrast to the initial receiving sets manufactured in the mid-1970s as part of the system concept validation phase. These first receivers were primarily analog devices for military applications and were large, bulky, and heavy. Today, receivers take on many form factors, including chipsets, handheld units, and Industry Standard Architecture (ISA) compatible cards. In fact, there are many single-chip GPS receivers that have leveraged low-voltage bipolar complementary metal oxide semiconductor (BiCMOS) processes and power-management techniques to meet the need for small size and low battery drain of handheld devices. Selection of a GPS receiver depends on the user's application (e.g., civilian versus military, platform dynamics, and shock and vibration environment). Following a description of a typical receiver's components, selection criteria are addressed. Detailed information regarding GPS receiver architectures and integrations for cellular telephone and automotive applications is contained in Chapter 9.

3.4.1 GPS Set Characteristics

A block diagram of a GPS receiving set is shown in Figure 3.23. The GPS set consists of five principal components: antenna, receiver, processor, input/output (I/O) device such as a control display unit (CDU), and a power supply.

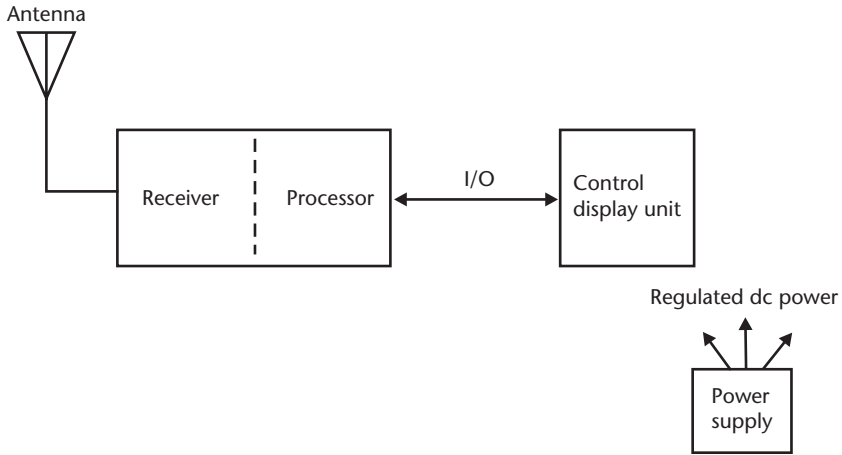


Figure 3.23 Principal GPS receiver components.

3.4.1.1 Antenna

Satellite signals are received via the antenna, which is right-hand circularly polarized (RHCP) and provides near hemispherical coverage. Typical coverage is 160° with gain variations from about 2.5 dBic at zenith to near unity at an elevation angle of 15°. (The RHCP antenna unity gain also can be expressed as 0 dBic = 0 dB with respect to an isotropic circularly polarized antenna.) Below 15°, the gain is usually negative. An example antenna pattern is shown in Figure 3.24. This pattern was pro-

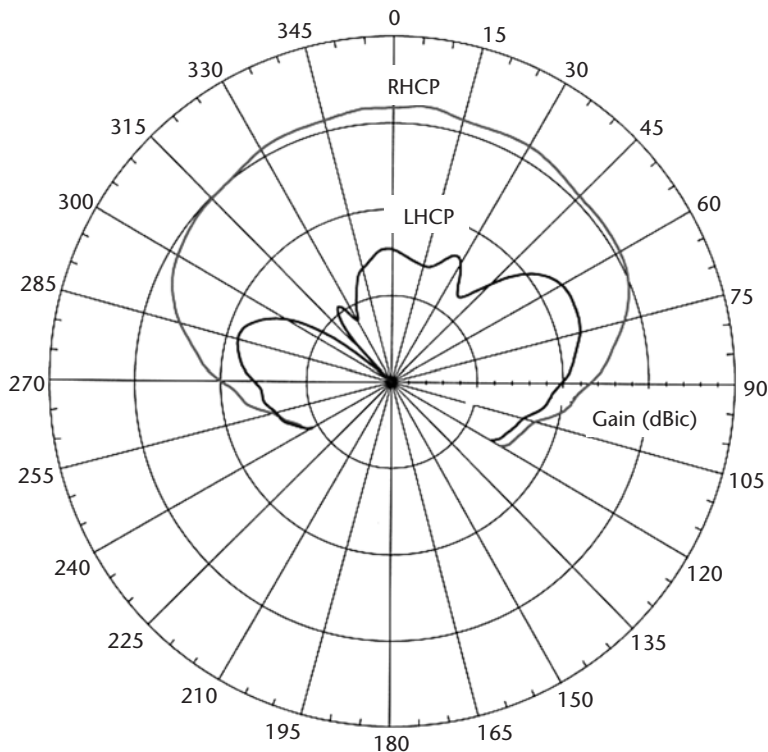


Figure 3.24 Example of RHCP hemispherical antenna pattern.

duced by a stacked-patch antenna element embedded in a dielectric substrate. This particular antenna is designed to operate at both L1 and L2, but only the L1 pattern has been provided for illustration. Even well-designed GPS antennas will exhibit a small but nonzero cross-polarized left-hand circularly polarized (LHCP) response in addition to the desired RHCP pattern shown in Figure 3.24. It can be observed that the RHCP response is nearly perfect at boresight, but as the elevation angle decreases the response is attenuated (i.e., the antenna gain decreases). This gain decrease is attributed to the horizontal electric field component being attenuated by the conducting ground plane. Therefore, a typical GPS antenna tends to be predominantly vertically polarized for low elevation angles. At zenith, the ratio of the vertical electric field to the horizontal electric field response is near unity. This ratio is referred to as the axial ratio. As the elevation angle decreases, the axial ratio increases.

Another GPS antenna design factor is transfer response. So that the signal is undistorted, it is desirable for the magnitude response to be nearly constant as a function of frequency and for the phase response to be linear with frequency within the passband of interest. (GPS signal bandwidths are discussed later as well as in Chapter 4.)

Furthermore, when we compute position with a GPS receiver, we are truly estimating the position of the electrical phase center of the antenna. There is both a physical and an electrical realization of this phase center. The physical realization is just that. One can actually use a ruler to measure the physical center of the antenna. However, the electrical phase center is often not collocated with the physical phase center and may vary with the direction of arrival of the received signal. The electrical and physical phase centers for survey-grade GPS antennas may vary by centimeters. Calibration data describing this difference may be required for high-accuracy applications.

Finally, a low-noise amplifier may be embedded in the antenna housing (or radome) in some GPS antennas. This is referred to as an active antenna. The purpose of this is to maintain a low-noise figure within the receiver. One must note that the amplifier requires power, which is usually supplied by the receiver front end thru the RF coaxial cable.

The antenna (and receiver front end) must have sufficient bandwidth to pass the signals of interest. Typically, the bandwidth of a GPS patch or helix antenna ranges from 1% to 2% of the center frequency. Two percent bandwidths for L1, L2, and L5 center frequencies are 31.5 MHz, 24.6 MHz, and 23.5 MHz, respectively. GPS receivers that track P(Y) code on both L1 and L2 need to accommodate on the order of 20.46-MHz bandwidths on both frequencies. If the set only tracks C/A code or L1C on L1, the antenna (and receiver) need to accommodate bandwidths of approximately 2.046 and 4.092 MHz, respectively. It should be noted that the receiver's antenna/front-end bandwidth is directly proportional to the accuracy required for the specific application of the receiver. That is, the more frequency content of the received satellite signal that is processed, the better the accuracy performance will be. For example, a survey receiver antenna/front end will most likely be designed to pass the full 20.46 MHz of the P(Y) code. Whereas, a low-cost hiking receiver designed for C/A code may only have a front-end bandwidth of 1.7 MHz instead of the full 2.046 MHz. (Further elaboration on bandwidth and accuracy performance is contained in Chapter 5.)

New civil signals L2C and L5 have null-to-null bandwidths of 2.046 MHz and 20.46 MHz, respectively. The military M code can be processed within the existing L1 and L2 24-MHz bandwidths. Since M code signal power is defined within a 30.69-MHz band around the center frequency, approximately 92% of this power is within the 24-MHz band. (GPS signal characteristics are contained in Chapter 4.)

The addition of new signals (M code, L1C, L2C, and L5) will require new antennas for some users. For example, those utilizing L1 C/A code and L2C will need a dual-band antenna. (Dual frequency measurements enable determination of the ionospheric delay and provide robustness to interference. Ionospheric delay determination and compensation are discussed in Chapter 7.) SOL signal users that require operation in the ARNS bands will need antennas to receive C/A code on L1 and the L5 signal on L5. At the time of this writing, RTCA was developing aviation standards for a dual-band L1/L5 antenna. Some receivers may be tri-band. That is, they will receive and process the signals broadcast on all three GPS frequencies, L1, L2, and L5, which will require a tri-band antenna. Reference [33] provides details on one approach for a tri-band (L1/L2 M code and L5) antenna design.

Antenna designs vary from helical coils to thin microstrip (i.e., patch) antennas. High-dynamic aircraft prefer low-profile, low-air resistance patch antennas, whereas land vehicles can tolerate a larger antenna. Antenna selection requires evaluation of such parameters as antenna gain pattern, available mounting area, aerodynamic performance, multipath performance, and stability of the electrical phase center of the antenna [34].

Another issue regarding antenna selection is the need for resistance to interference. (In the context of this discussion, any electronic emission, whether friendly or hostile, that interferes with the reception and processing of GPS signals is considered an interferer.) Some military aircraft employ antenna arrays to form a null in the direction of the interferer. Another technique to mitigate the effects of interference is to employ a beam-steering array. Beam-steering techniques electronically concentrate the antenna gain in the direction of the satellites to maximize link margin. Finally, beam forming combines both nulling and beam steering for interferer mitigation. (References [35–37] provide detailed descriptions of the theory and practical applications of nulling, beam steering, and beam forming.)

3.4.1.2 Receiver

Chapter 5 provides a detailed description of receiver signal acquisition and tracking operation; however, some high-level aspects are described herein to aid our discussion. Two basic receiver types exist today: (1) those that track L1 C/A code and P(Y) code on L1 and L2 and (2) those that only track C/A code. In light of the GPS modernization effort, these are referred to as legacy receivers. Forthcoming military receivers are being referred to as YMCA. That is, they will track L1 C/A, L1 and L2 P(Y), and L1 and L2 M code. The forthcoming civil signals, L1C, L2C, and L5, will require new receivers to be built. It is envisioned that a number of receiver types will be available. Most likely, these will be dual band to achieve ionospheric compensation and increased interference immunity. As mentioned earlier, ARNS band users will require dual band (L1 and L5) receivers and antennas.

Legacy PPS users generally employ sets that track P(Y) code on both L1 and L2. These sets initiate operation with receivers tracking C/A code on L1 and then transition to tracking P(Y) code on both L1 and L2. Y-code tracking occurs only with the aid of cryptographic equipment. (If the satellite signal is encrypted and the receiver does not have the proper cryptographic equipment, the receiver generally defaults to tracking C/A code on L1.) It is anticipated that the forthcoming YMCA receivers will perform a direct acquisition of the M code signal. Following M code acquisition, the receivers will then track M code on both L1 and L2 if the receiver is capable of dual-frequency operation. Otherwise, it will operate on either L1 or L2.

Alternatively, legacy SPS users employ sets that track the C/A code exclusively on L1, since that is the only frequency on which the C/A code is generally broadcast. Forthcoming L1C, L2C, and L5 receivers will track signals on these respective frequencies.

In addition to the receiver types mentioned earlier, there are other variations, such as civilian semicodeless tracking receivers, which track the C/A code on L1 and carrier phase of both the L1 and L2 frequencies. These receivers employ signal-processing techniques that do not require cryptographic access to the P(Y) code. Utilizing the carrier phase as a measurement observable enables centimeter-level (or even millimeter-level) measurement accuracy. (Carrier-phase measurements are described extensively in Section 8.4.) Most receivers have multiple channels whereby each channel tracks the transmission from a single satellite. A simplified block diagram of a multichannel generic SPS receiver is shown in Figure 3.25. The

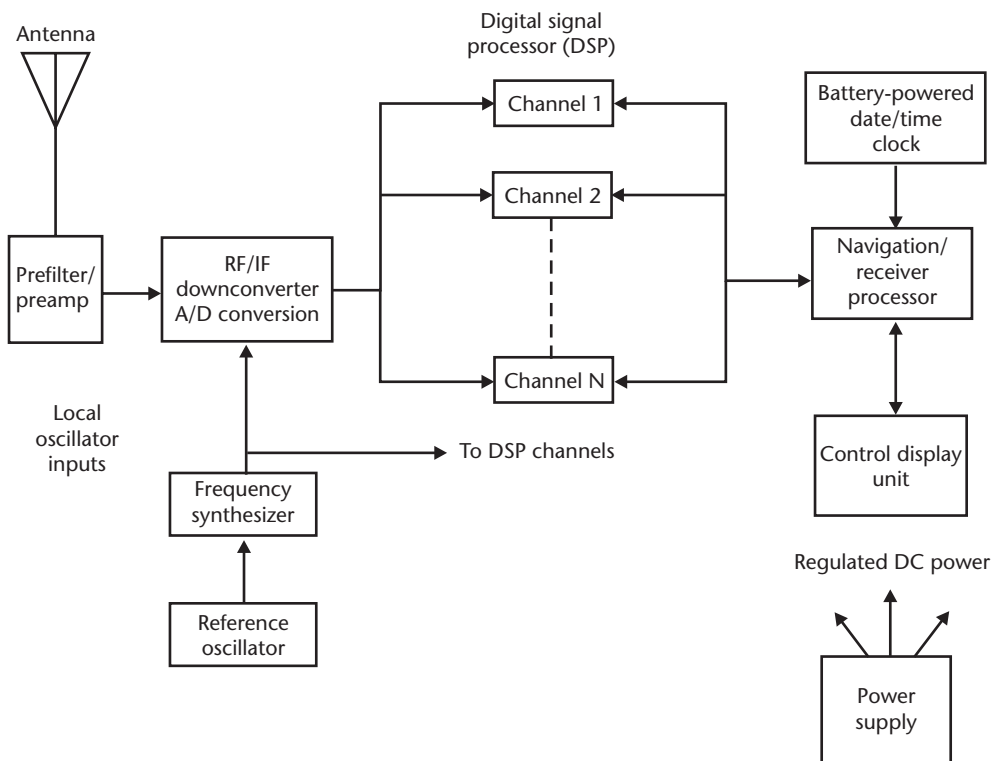


Figure 3.25 Generic SPS receiver.

received RF CDMA satellite signals are usually filtered by a passive bandpass prefilter to reduce out-of-band RF interference.

This is normally followed by a preamplifier. The RF signals are then downconverted to an intermediate frequency (IF). The IF signals are sampled and digitized by an analog to digital (A/D) converter. The A/D sampling rate is typically 2 to 20 times the PRN code chipping rate [1.023 MHz for L1 C/A code and 10.23 MHz for L1 and L2 P(Y) code]. The minimum sampling rate is twice the stopband bandwidth of the codes to satisfy the Nyquist criterion. For L1 C/A code only sets, the stopband bandwidth may be slightly greater than 1 MHz. Alternatively, the stopband bandwidth is slightly more than 10 MHz for P(Y) code sets. Oversampling reduces the receiver sensitivity to A/D quantization noise, thereby reducing the number of bits required in the A/D converter. The samples are forwarded to the digital signal processor (DSP). The DSP contains N parallel channels to simultaneously track the carriers and codes from up to N satellites. (N generally ranges from 8 to 12 in today's receivers.) Each channel contains code and carrier tracking loops to perform code and carrier-phase measurements, as well as navigation message data demodulation. The channel may compute three different satellite-to-user measurement types: pseudoranges, delta ranges (sometimes referred to as delta pseudorange), and integrated Doppler, depending on the implementation. The desired measurements and demodulated navigation message data are forwarded to the processor.

Note that GPS receivers designed for use in handheld devices need to be power efficient. Depending on the implementation, these receivers may trade off susceptibility to high-power in-band interferers to achieve minimum power supply (e.g., battery) drain. High dynamic range receiver front ends are needed in interference-resistant receivers, and the necessary components (e.g., amplifiers and mixers with high intermodulation product levels) require high bias voltage levels.

3.4.1.3 Navigation/Receiver Processor

A processor is generally required to control and command the receiver through its operational sequence, starting with channel signal acquisition and followed by signal tracking and data collection. (Some GPS sets have an integral processing capability within the channel circuitry to perform these signal-processing functions.) In addition, the processor may also form the PVT solution from the receiver measurements. In some applications, a separate processor may be dedicated to the computation of both PVT and associated navigation functions. Most processors provide an independent PVT solution on a 1-Hz basis. However, receivers designated for autoland aircraft precision approach and other high-dynamic applications normally require computation of independent PVT solutions at a minimum of 5 Hz. The formulated PVT solution and other navigation-related data is forwarded to the I/O device.

3.4.1.4 I/O Device

The I/O device is the interface between the GPS set and the user. I/O devices are of two basic types: integral or external. For many applications, the I/O device is a

CDU. The CDU permits operator data entry, displays status and navigation solution parameters, and usually accesses numerous navigation functions, such as waypoint entry and time to go. Most handheld units have an integral CDU. Other installations, such as those onboard an aircraft or ship, may have the I/O device integrated with existing instruments or control panels. In addition to the user and operator interface, applications such as integration with other sensors (e.g., INS) require a digital data interface to input and output data. Common interfaces are ARINC 429, MIL-STD-1553B, RS-232, and RS-422.

3.4.1.5 Power Supply

The power supply can be either integral, external, or a combination of the two. Typically, alkaline or lithium batteries are used for integral or self-contained implementations, such as handheld portable units; whereas an existing power supply is normally used in integrated applications, such as a board-mounted receiver installed within a server to provide accurate time. Airborne, automotive, and ship-board GPS set installations normally use platform power but typically have built-in power converters (ac to dc or dc to dc) and regulators. There usually is an internal battery to maintain data stored in volatile random access memory (RAM) integrated circuits (ICs) and to operate a built-in timepiece (date/time clock) in the event platform power is disconnected.

3.4.2 GPS Receiver Selection

At the time of this writing, there were well over 100 GPS set manufacturers in the United States and abroad. While some, like SiRF, offer a few different chip set receivers for integration with other electronic functions, other companies like GARMIN and Trimble Navigation have many different end products ranging from handhelds to automobile and aircraft navigators to complex survey receivers. GPS receiver selection is dependent on user application. The intended application strongly influences receiver design, construction, and capability. For each application, numerous environmental, operational, and performance parameters must be examined. A sampling of these parameters follows:

- What are the shock and vibration requirements, temperature and humidity extremes, as well as atmospheric salt content?
- If the receiver is to be used by government or military personnel, PPS operation may be required. PPS operation usually dictates that a dual-frequency set with a cryptographic capability is needed.
- The necessary independent PVT update rate must be determined. As an example, this rate is different for aircraft precision approach than it is for marine oil tanker guidance.
- Will the receiver have to operate in a high-multipath environment (i.e., near buildings or on an aircraft where satellite signals are reflected by various fuselage surfaces)? If so, multipath mitigation signal-processing techniques may be required. (Detailed descriptions of multipath and multipath-mitigation

techniques are contained in Chapter 6. The contribution to the GPS error budget is described in Chapter 7.)

- Under what type of dynamic conditions (e.g., acceleration and velocity) will the set have to operate? GPS sets for fighter aircraft applications are designed to maintain full performance even while experiencing multiple “Gs” of acceleration, whereas sets designated for surveying are not normally designed for severe dynamic environments.
- Is a DGPS capability required? (DGPS is an accuracy-enhancement technique covered in Chapter 8.) DGPS provides greater accuracy than stand-alone PPS and SPS. Most receivers are manufactured with a DGPS capability.
- Does the application require reception of the geostationary satellite-based overlay service referred to as SBAS broadcasting satellite integrity, ranging, and DGPS information? (SBAS is discussed in Chapter 8.)
- Waypoint storage capability as well as the number of routes and legs need to be assessed.
- Does the GPS set have to operate in an environment that requires enhanced interference rejection capabilities? Chapter 6 describes several techniques to achieve this.
- If the receiver has to be interfaced with an external system, does the proper I/O hardware and software exist? An example would be a user who requires a blended solution consisting of GPS and other sensors, such as an IMU and vision system.
- In terms of data input and display features, does the receiver require an external or integral CDU capability? Some aircraft and ships use *repeater* units such that data can be entered or extracted from various physical locations. Display requirements such as sunlight-readable or night-vision-goggle-compatible must be considered.
- Are local datum conversions required, or is WGS-84 sufficient? If so, does the receiver contain the proper transformations?
- Is portability for field use required?
- Economics, physical size, and power consumption must also be considered.

As stated earlier, these are only a sampling of GPS set selection parameters. One must carefully review the requirements of the user application prior to selecting a receiver. In most cases, the selection will be a tradeoff that requires awareness of the impact of any GPS set deficiencies for the intended application.

References

- [1] Bates, R., et al., *Fundamentals of Astrodynamics*, New York: Dover Publications, 1971.
- [2] U.S. Department of Defense, *Global Positioning System Standard Positioning Service Performance Standard*, Washington, D.C., October 2001.
- [3] U.S. Coast Guard Navigation Center, <http://www.navcen.uscg.gov>.
- [4] Riley, W. J., *Rubidium Atomic Frequency Standards for GPS Block IIR*, ION-GPS-92, Albuquerque, NM, September 1992.

- [5] Marquis, W., "Increased Navigation Performance from GPS Block IIR," *NAVIGATION: Journal of The Institute of Navigation*, Vol. 50, No. 4, Winter 2003–2004.
- [6] Taylor, J., and E. Barnes, "GPS Current Signal-In-Space Performance," *ION 2005 Annual Technical Meeting*, San Diego, CA, January 24–26, 2005.
- [7] Marquis, W., and C. Krier, *Examination of the GPS Block IIR Solar Pressure Model*, ION-GPS-2000, Salt Lake City, UT, September 2000.
- [8] Swift, E. R., *GPS REPORTS: Radiation Pressure Scale and Y-Axis Acceleration Estimates for 1998–1999*, Naval Surface Warfare Center, report #3900 T10/006, March 9, 2000.
- [9] Hartman, T., et al., "Modernizing the GPS Block IIR Spacecraft," *ION-GPS-2000*, Salt Lake City, UT, September 2000.
- [10] Marquis, W., "M Is for Modernization: Block IIR-M Satellites Improve on a Classic," *GPS World Magazine*, Vol. 12, No. 9, September 2001, pp. 38–44.
- [11] Parkinson, B., et al., *Global Positioning System: Theory and Applications*, Vol. I, Washington, D.C.: American Institute of Aeronautics and Astronautics, 1996.
- [12] Brown, K., et al., "L-Band Anomaly Detection in GPS," *Proc. of the 51st Annual Meeting, Inst. of Navigation*, Washington, D.C., 1995.
- [13] Hay, C., and J. Wong, "Improved Tropospheric Delay Estimation at the Master Control Station," *GPS World*, July 2000, pp. 56–62.
- [14] Mendicki, P., "GPS Ground Station Coverage—Visibility Gap Analysis," Aerospace Corporation, October 2002, unpublished.
- [15] "GPS OCS Mathematical Algorithms, Volume GOMA-S," DOC-MATH-650, Operational Control System of the NAVSTAR Global Positioning System, June 2001.
- [16] Cappelleri, J., C. Velez, and A. Fucha, *Mathematical Theory of the Goddard Trajectory Determination System*, Goddard Space Flight Center, April 1976.
- [17] Springer, T., *Modeling and Validating Orbits and Clocks Using the Global Positioning System*, Ph.D. Dissertation, Astronomical Institute, University of Bern, November 1999.
- [18] Maybeck, P. S., *Stochastic Models, Estimation and Control*, Vol. 1, New York: Academic Press, 1979.
- [19] Bierman, G. J., *Factorization Methods for Discrete Sequential Estimation*, Orlando, FL: Academic Press, 1977.
- [20] "GPS OCS Mathematical Algorithms, Volume GOMA-E," DOC-MATH-650, Operational Control System of the NAVSTAR Global Positioning System, June 2001.
- [21] Buisson, J., "NAVSTAR Global Positioning System: Quarterly Reports," Naval Research Laboratory, Quarterly, Washington, D.C., July 31, 2004.
- [22] Van Dierendonck, A., and R. Brown, "Relationship Between Allan Variances and Kalman Filter Parameters," *Proc. of 16th Annual PTTI Meeting*, Greenbelt, MD, 1984.
- [23] Hopfield, H., "Tropospheric Effects on Electromagnetically Measured Range, Prediction from Surface Water Data," *Radio Science*, Vol. 6, No. 3, March 1971, pp. 356–367.
- [24] Black, H., "An Easily Implemented Algorithm for Tropospheric Range Correction," *Journal of Geophysical Research*, Vol. 83, April 1978, pp. 1825–1828.
- [25] Brown, K., "The Theory of the GPS Composite Clock," *Proc. of ION GPS-91*, Institute of Navigation, Washington, D.C., 1991.
- [26] Senior, K., et al., "Developing an IGS Time Scale," *IEEE Trans. on Ferroelectrics and Frequency Control*, June 2003, pp. 585–593.
- [27] Brown, K., et al., "Dynamic Uploading for GPS Accuracy," *Proc. of ION GPS-97*, Institute of Navigation, Washington, D.C., 1997.
- [28] Yinger, C., et al., "GPS Accuracy Versus Number of NIMA Stations," *Proc. of ION GPS 03*, Institute of Navigation, Washington, D.C., 2003.
- [29] McCarthy, D., (ed.), *IERS Technical Note*, 21, U.S. Naval Observatory, July 1996.
- [30] Bar-Sever, Y., and D. Kuang, "New Empirically Derived Solar Radiation Pressure Model for GPS Satellites," *JPL Interplanetary Network Progress Report*, Vol. 24-159, November

- 2004; addendum: “New Empirically Derived Solar Radiation Pressure Model for Global Positioning System Satellites During Eclipse Seasons,” *JPL Interplanetary Network Progress Report*, Vol. 42-160, February 2005.
- [31] Saastamoinen, J., “Contributions to the Theory of Atmospheric Refraction,” *Bulletin Géodésique*, No. 105, pp. 270–298; No. 106, pp. 383–397; No. 107, pp. 13–34, 1973.
- [32] Niell, A., “Global Mapping Functions for the Atmosphere Delay at Radio Wavelengths,” *Journal of Geophysical Research*, Vol. 101, No. B2, 1996, pp. 3227–3246.
- [33] Rama Rao, B., et al., “Triple Band GPS Trap Loaded Inverted L Antenna Array,” The MITRE Corporation, 2002, http://www.mitre.org/work/tech_papers/tech_papers_02/rao_triband.
- [34] Seeber, G., *Satellite Geodesy: Foundations, Methods, and Applications*, New York: Walter De Gruyter, 1993.
- [35] Klemm, R., *Principles of Space-Time Adaptive Processing*, London: The Institution of Electrical Engineers, 2002.
- [36] Klemm, R., *Applications of Space-Time Adaptive Processing*, London: The Institution of Electrical Engineers, 2004.
- [37] Fante, R., and J. Vaccaro, “Wideband Cancellation of Interference in a GPS Receive Array,” *IEEE Trans. on Aerospace and Electronic Systems*, Vol. AES-36, April 2000, pp. 549–564.